Coordination Chemistry Reviews 255 (2011) 1226–1251

Contents lists available at ScienceDirect

Coordination Chemistry Reviews

journal homepage: www.elsevier.com/locate/ccr

Review

The structures of lithium and magnesium organocuprates and related species

Robert P. Davies*

Department of Chemistry, Imperial College London, Exhibition Road, South Kensington, London SW7 2AZ, UK

Contents

ARTICLE INFO

Article history:
Received 2 November 2010
Accepted 3 January 2011
Available online 8 January 2011

Keywords:
Copper(I)
Lithium
Magnesium
X-ray structures
Addition reactions

ABSTRACT

Organocuprates are excellent reagents for the formation of carbon–carbon bonds and have been used extensively in synthetic methodology for over fifty years. However, despite their long pedigree the structures, solution behavior, and mechanism of operation of these reagents have often remained opaque. This review concentrates upon the resting-state structures of organocuprates as determined using X-ray crystallographic studies, and provides a comprehensive survey of all solid-state structural characterizations of these species and the intricate nature of their supramolecular assemblies. In addition, solution state experimental data is also presented where it pertains directly to the presented solid-state structures or where it illustrates key points crucial to the understanding of organocuprate reactivity. The structures of all the main classes of organocuprate reagent will be discussed including lithium and magnesium homo-cuprates, cyano-cuprates and hetero-cuprates.

1. Introduction

The chemistry of organocopper compounds, that is to say coordination complexes consisting of one or more organic groups such as an alkyl or aryl bound to a copper metal center, can be traced back to the early part of the twentieth century and the first reported synthesis of phenyl copper (PhCu) by Reich and Hebd [1]. Although copper is known to adopt a range of oxidation states from 0 to +4, the organometallic chemistry of copper is predominately associated with the +1 oxidation state (and also to a lesser extent the +3 oxidation state). In contrast, organometallic copper(II) compounds are on the whole intrinsically unstable, either undergoing reductive elimination to give copper(0) and cross-coupling of the organo groups, or decomposition to give an organic radical.

One of the main driving factors in the development and study of organocopper chemistry over the past century has been the application of these species in organic synthesis. The potential utility of organocopper compounds in the field of synthesis was first

* Tel.: +44 20 75945754.
E-mail address: r.davies@imperial.ac.uk

0010-8545/$ – see front matter © 2011 Elsevier B.V. All rights reserved.
doi:10.1016/j.ccr.2011.01.011

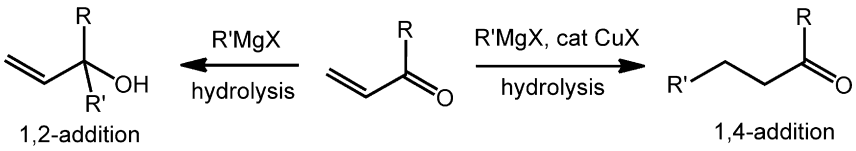

Scheme 1. The addition reactions of Grignard reagents.

identified by Gilman in 1936 when he reported upon the ability of organocopper(I) compounds to undergo coupling reactions with organo-halides [2]. Soon afterwards Kharasch and Tawney demonstrated how small amounts of copper salts could catalyze the 1,4-addition of Grignard reagents to α,β-unsaturated ketones, thus contrasting with the 1,2-addition reaction which was observed in the absence of any copper salt (see Scheme 1) [3]. Such conjugate addition reactions are today synonymous with organocuprate chemistry.

A seminal moment in the development of organocopper chemistry was the first reported synthesis of an organocuprate by Gilman in 1952 [4]. Gilman demonstrated how the addition of one equivalent of methyllithium to one equivalent of cuprous iodide gave an ether-insoluble organocopper(I) product, methyl copper, which when treated with a second equivalent of methyllithium redissolved to give a new soluble product, lithium dimethylcuprate (see Scheme 2).

Despite some early successes [2], organocopper (RCu) reagents were found to suffer from several shortcomings which severely limited their adoption for organic synthesis protocols. Problems associated with organocopper reagents included low solubility, low reactivity and high thermal instability (for example methylcopper is highly explosive when dry [5]). However, R_2CuLi organocuprate species (or Gilman reagents as they later became known), were shown to have significantly higher solubility (especially in ethereal solvents), increased reactivity and less thermally explosive decomposition pathways (although careful handling and a thorough appreciation of the risks is still required, particularly for the methyl variants). These advantageous properties proved key to the development of hetero-metallic organocuprates, such as R_2CuLi and R_2CuMgX, in organic synthesis.

Pioneers in demonstrating the synthetic capability of organocuprates were House, Corey and Whitesides whose initial work in the 1960s [6–8] quickly led to the widespread adoption of organocuprates for a range of carbon–carbon bond-forming reactions. These reactions included, but were not limited to, substitution reactions, coupling reactions, conjugate addition and carbocupration. Nowadays, organocuprates are firmly established as one the key organometallic reagents in the synthetic toolbox of the organic chemist. The numerous current applications of organocuprates and related species in synthesis protocols are beyond the scope of this review, but have been extensively documented in the literature elsewhere [9–13].

Today the term organocuprate covers a diverse range of compounds encompassing not just the original "R_2CuLi" Gilman organocuprates, but also organocuprates with varying stoichiometric R:Cu:Li ratios, heteroleptic organocuprates with heteroatom-based as well as organo-based R groups, organocuprates modulated by the addition of neutral ligands or other additives, and organocuprates with a range of hetero metal centers beyond just lithium or magnesium. This expansion of structural diversity has been prompted by the desire to improve the reactivity, stability, and efficiency of these reagents as well to optimize their chemo-, regio- and stereo-selectivity.

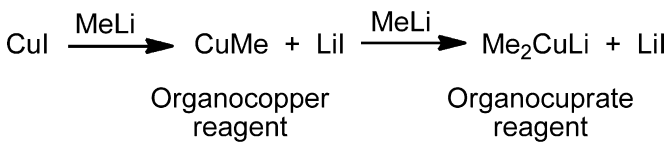

Scheme 2. The synthesis of organocopper and organocuprate reagents.

Developments in the field of organocuprates have mostly taken place empirically, that is to say by practical experimentation rather than rational design. For many years organocuprates were, and in some cases still are, referred to as 'black box' reagents, thus reflecting the lack of knowledge concerning their structures, mode of operation and often even the constituent components of their active species. Indeed, structural and characterizational studies on organocuprates and their reaction intermediates have frequently been hampered by the thermal instability of these species, as well as their high sensitivity to oxygen and moisture. In addition, organocuprates can exhibit complex behavior in solution, often existing as a number of different species in equilibrium, thus further complicating their characterization. However, despite these problems, significant advances have been made in the understanding of organocuprates using a range of structural (both solid state and solution), computational and kinetic studies. Simple, unfunctionalized Gilman cuprates in particular have been extensively investigated in this context, providing many critical insights into the nature of these species and the origins of their unique reactivity.

This review focuses upon the structures of lithium and magnesium organocuprates, and in particular the advances made during the last decade which have not been covered in earlier reviews [14–17]. The main emphasis will be on the solid-state structures of lithium and magnesium organocuprates. Although solid-state structural determination has often proven to be a key first step to our understanding of organocuprates and related species, it should be noted that the solid-state structures which crystallize are often the most thermodynamically stable species (resting-state species) and therefore may not reflect the different solution structures or indeed the most reactive species. Therefore, NMR spectroscopic and other solution-state characterization techniques, along with computational and kinetic studies, are also crucial to unraveling the chemistry of organocuprates. Hence in this review, solution characterization and other experimental data will also be presented where it illustrates key points or where it pertains directly to the presented solid-state structures. For a more comprehensive account of the NMR structure elucidation of copper based reagents, including organocuprates, the reader is directed to a recent review by Gschwind [18].

2. Lithium homocuprates

Homocuprates are homoleptic complexes in which all the anionic ligands (R groups) bound to the copper center are identical. The simplest of these, lithium diorganocuprates, adhere to the stoichiometry R_2CuLi and are formed in the reaction of one equivalent of a copper(I) halide with two equivalents of organolithium reagent as first proposed by Gilman (Scheme 2). However, even the structures of these simplest organocuprates can vary significantly depending upon the nature of the organo R group, the solvent system, and the presence of other additives or by-products such as lithium halides. In addition, variation of the copper to lithium ratio

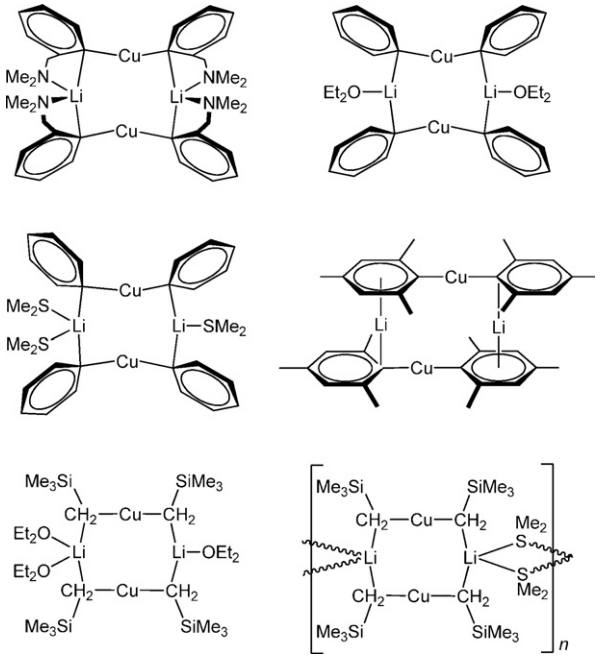

Fig. 1. Crystallographically characterized dimeric lithium homo-cuprates.

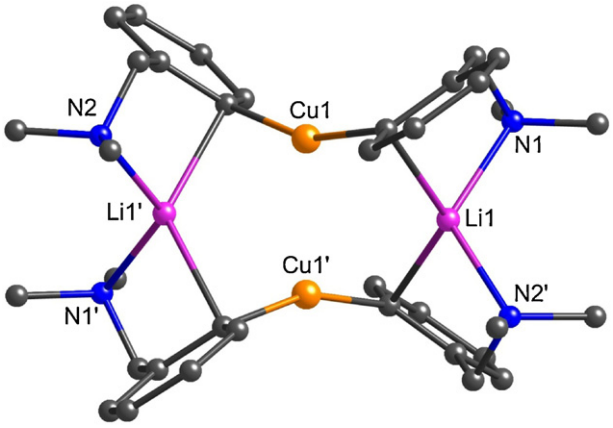

Fig. 2. Molecular structure of $[Cu_2Li_2(C_6H_4CH_2NMe_2\text{-}2)_4]_2$ [25].

can lead to radically different structural motifs and can also have a large effect on the reactivity of these reagents.

2.1. Lithium diorganocuprate aggregates $(R_2CuLi)_n$

The most thermodynamically stable form, or resting state, of lithium diorganocuprates (at least in non- or weakly-coordinating solvents) is now commonly accepted to be a dimeric aggregate based upon an eight-membered cyclic structure in which the aryl or alkyl groups bridge the copper and lithium atoms. A number of lithium diorganocuprates have been characterized in the solid-state which conform to this structural motif (Fig. 1).

Given that lithium diorganocuprates were amongst the first organocuprate compounds to be subject to structural characterization – initially in solution, and then following advances in X-ray crystallography in the solid state – it is worthwhile considering the chronology of developments in this area.

Not long after the first reports concerning the synthetic utility of organocuprates in organic transformations were published, attempts were initiated to investigate the structures of these reagents and their mechanism of reaction with organic substrates. Initially research focused upon simple alkyl and aryl derivatives (R = Me or Ph) in weakly coordinating solvents such as Et_2O. Thus the homocuprate $[Me_2CuLi]_n$ was studied in diethyl ether solution using vapor pressure depression measurements, ^{1}H NMR spectroscopy, and solution X-ray scattering, all of which pointed towards a dimeric structure ($n = 2$) with D_{2h} symmetry [19]. The existence of such a dimeric aggregate was also congruent with kinetic measurements on the reaction of Me_2CuLi with MeI [19]. A similar dimeric aggregate was also thought to be formed in the reaction of $LiCH_2SiMe_3$ with $CuCH_2SiMe_3$: despite varying the ratio of organolithium to organocopper reagents, ^{1}H NMR studies indicated that the only heterobimetallic species formed was the 1:1 Cu:Li species in all cases [20,21].

One of the first homocuprates to be isolated in high purity was the diarylcuprate $[Cu_2Li_2(C_6H_4CH_2NMe_2\text{-}2)_4]$ in which the aryl groups are functionalized with dimethylamino substituents capable of coordinating to the metal atoms *via* their nitrogen lone pair. Crysoscopic molecular weight determinations in benzene indicated a dimeric aggregate was once more predominate [22], and this was reinforced both by detailed NMR spectroscopic studies and also by comparison with its silver and gold homologs $[M_2Li_2(C_6H_4CH_2NMe_2\text{-}2)_4]$ (M = Ag, Au) [23,24]. Together these results allowed the authors to propose a structure in which each aryl group bridges one copper and one lithium atom *via* the *ipso*-carbon, thus giving rise to a dimeric eight-membered cyclic structure. Later, single crystal X-ray structural studies revealed such a dimeric aggregate also to be present in the solid state (Fig. 2) [25]. In agreement with the predicted solution structure, the aryl groups in the solid-state structure of $[Cu_2Li_2(C_6H_4CH_2NMe_2\text{-}2)_4]_2$ each asymmetrically bridge a lithium and a copper to give a cyclic structure in which the lithium centers are tetra-coordinate to two bridging *ipso*-carbons and two dimethylamino groups. The copper centers in $[Cu_2Li_2(C_6H_4CH_2NMe_2\text{-}2)_4]_2$ are two-coordinate with a reported C–Cu–C angle of 157.7(1)° and a Cu–C_{ipso} distance of 1.942(3) Å. Although the Li–C_{ipso} bond distance is much longer at 2.385(6) Å, some degree of covalent character can be inferred from the tilting of the aryl groups towards the lithium and from the observation in solution of a $^1J(^{13}C_{ipso}, ^7Li)$ coupling constant of 7 Hz [25].

The potential role of the *ortho*-CH_2NMe_2 groups in $[Cu_2Li_2(C_6H_4CH_2NMe_2\text{-}2)_4]_2$ towards dimer formation was explored by comparison with the unfunctionalized diarylcuprate $[Cu_2Li_2(C_6H_4CH_3\text{-}4)_4(OEt_2)_2]$. Solution ^{1}H NMR and molecular mass measurements again indicated dimeric aggregates were present, despite the absence of any pendant donor groups [26]. Moreover, crystal structure determinations of the diphenylcuprates $[Cu_2Li_2Ph_4(OEt_2)_2]$ [27] and $[Cu_2Li_2Ph_4(SMe_2)_3]$ [28] yielded similar dimeric structures, differing only in the degree of solvation of the lithium cation (Fig. 3). In $[Cu_2Li_2Ph_4(OEt_2)_2]$ each lithium cation is solvated by one solvent molecule (Et_2O) to give a trigonal coordination, whereas in $[Cu_2Li_2Ph_4(SMe_2)_3]$ one of the lithium cations is tri-coordinate to one dimethyl sulfide (DMS) molecule and two phenyl *ipso*-carbons, whereas the other is four-coordinate to two *ipso*-carbons and two DMS molecules. The use of DMS in these studies stems from earlier work showing organocuprate reagents to be both more stable and more reactive when prepared in DMS instead of diethyl ether or tetrahydrofuran [29].

Closer inspection of the solid-state structure of $[Cu_2Li_2Ph_4(OEt_2)_2]$ (Fig. 3a) [27] reveals some of the key bonding interactions present in these species. The complex can best be considered as two Ph_2Cu cuprate anions held together by the two lithium cations. The aryl groups each asymmetrically bridge a copper and lithium metal center at the *ipso*-carbon. The Cu–C_{ipso} distances (mean 1.918 Å) are shorter than those observed in similar

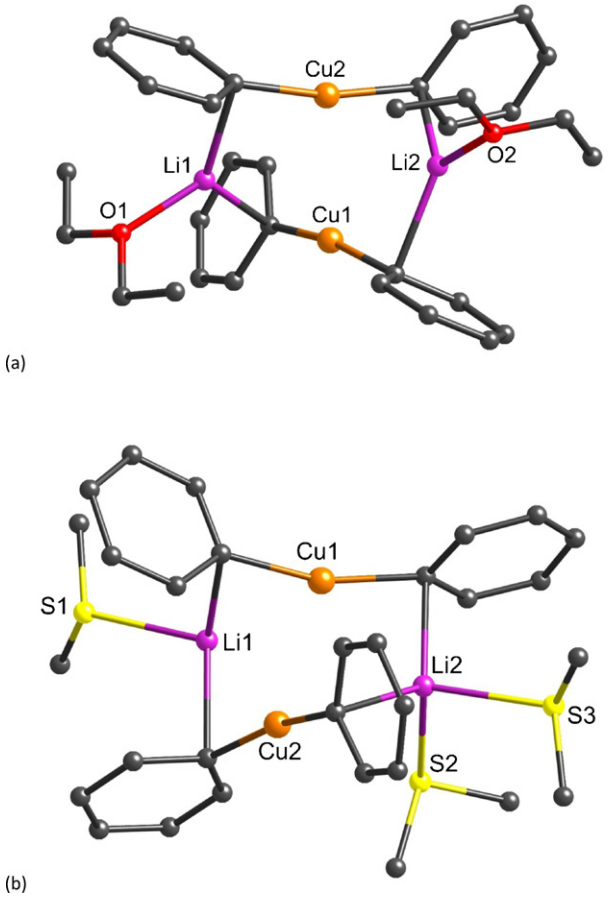

Fig. 3. Molecular structures of (a) $[Cu_2Li_2Ph_4(OEt_2)_2]$ [27] and (b) $[Cu_2Li_2Ph_4(SMe_2)_3]$ [28].

phenylcopper aggregates such as $[Cu_4Ph_4(SMe_2)_2]$ (mean 2.003 Å) [28], and the Li–C_{ipso} distances (mean 2.252 Å) are comparable to those in $[LiPh(Et_2O)]_4$ (mean 2.33 Å) [30]. Moreover, the two Ph_2Cu units in $[Cu_2Li_2Ph_4(OEt_2)_2]$ are approaching linearity (C–Cu–C, 163.2 to 168.0°), which compares to the less obtuse C–Cu–C angles (144.3 and 146.0°) observed in $[Cu_4Ph_4(SMe_2)_2]$. In these lithium diarylcuprates the aryl groups are therefore best considered to interact primarily *via* a σ-bonding interaction with the copper center, and by means of a weaker, predominately electrostatic interaction using a *p* or *π* orbital with the lithium atom. This contrasts to the much more symmetric aryl bridging observed in the arylcopper species, which can be regarded as forming essentially 3 center–2 electron Cu–C–Cu bonds.

The solid-state structure of the diarylcuprate $[Cu_2Li_2Mes_4]$ (Mes = $C_6H_2Me_3$-2,4,6) [31] also conforms to the dimeric motif. However, in this complex the absence of any solvent molecules or coordinating pendant groups on the aryl ring results in the lithium cations being effectively sandwiched between two coplanar mesityl groups (Fig. 4). Each lithium is η^6 coordinated to one aryl ring (mean Li–C = 2.316(4) Å) whilst sitting almost directly above (η^1) the *ipso*-carbon of another (Li–C_{ipso} = 2.129(4) Å). The absence of any other lithium coordinating units relaxes the steric requirements at the lithium center, thereby allowing the Mes_2Cu cuprate units to adopt a much closer-to-linear arrangement, C–Cu–C = 178.34(7)°, thus maximizing the Cu–C_{ipso} σ-bonding overlap (mean Cu–C_{ipso} 1.930(2) Å). Theoretical calculations indicate that the η^1,η^6 conformer observed in the solid state is also the most thermodynamically stable form of this complex. In addition, NMR spectroscopic studies are consistent with retention of

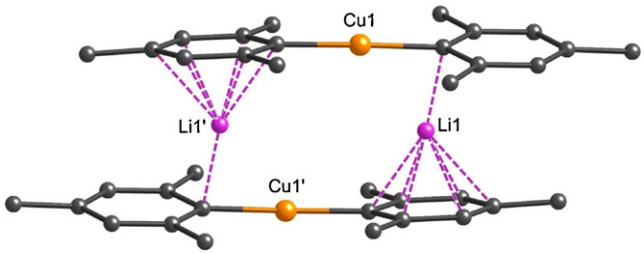

Fig. 4. Molecular structure of $[Cu_2Li_2(C_6H_2Me_3$-2,4,6$)_4]$ [31].

the same η^6,η^1 dimeric structure in benzene solution with only one singlet observed in the ^{7}Li spectra at −9.99 ppm. The unusually high chemical shift of this peak can be attributed to ring current phenomena, whereby the lithium sits in the magnetically anisotropic environment of the two aryl rings. It is salient to note that similar lithium η^6-aryl interactions have also been observed in the solid-state structure of solvent-free mesityllithium [32].

In addition to the diaryl cuprates described above, two dialkyl cuprate solid-state structures have also been reported, namely $[Cu_2Li_2(CH_2SiMe_3)_4(OEt_2)_3]$ [33] and $[Cu_2Li_2(CH_2SiMe_3)_4(SMe_2)_2]_\infty$ [34]. $[Cu_2Li_2(CH_2SiMe_3)_4(OEt_2)_3]$ adopts a similar dimeric structure to the previously discussed diarylcuprates. The sp^3 alkyl group asymmetrically bridges the Cu and Li centers with a mean Li–C distance of 2.270 Å and a mean Cu–C distance of 1.955 Å. The C–Cu–C angles of 171.3 and 172.9° are again approaching linearity, although in this structure the two R–Cu–R cuprate units are essentially orthogonal (93.7°) to one another (Fig. 5). Formal replacement of diethyl ether with the more weakly coordinating solvent dimethyl sulfide gives an unusual polymeric structure $[Cu_2Li_2(CH_2SiMe_3)_4(SMe_2)_2]_\infty$ [34]. Once more the dimeric motif is dominant, however in this case the sulfur atoms on two DMS molecules bridge the lithium atoms of adjacent dimers giving rise to four-membered Li_2S_2 rings (Fig. 6). This dialkyl cuprate is currently the only reported structurally characterized homocuprate $(RCuLi)_n$ to adopt an aggregation state (*n*) greater than two, however it is perhaps best considered as linked dimers rather than a true 'high aggregate' species. In addition, it seems likely that in solution excess dimethyl sulfide would break the polymeric structure down into smaller units [33]. It is interesting to note that similar 'aggregated dimer' structures have also been speculated to exist in lithium homocuprate solutions in diethylether, based on the results of NMR diffusion experiments which suggested molecular sizes larger than dimers [18,35].

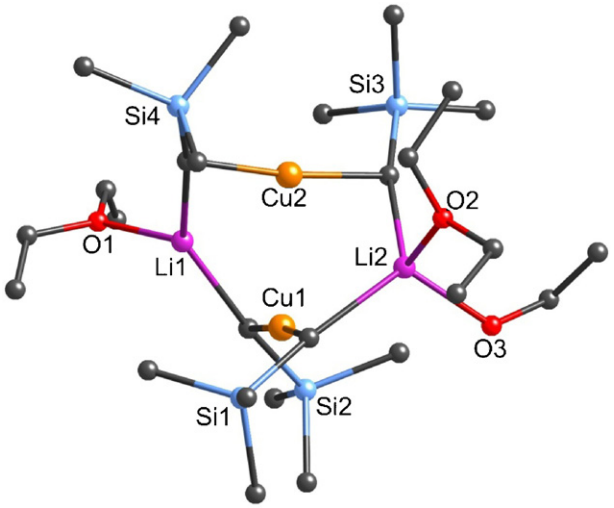

Fig. 5. Molecular structure of $[Cu_2Li_2(CH_2SiMe_3)_4(OEt_2)_3]$ [33].

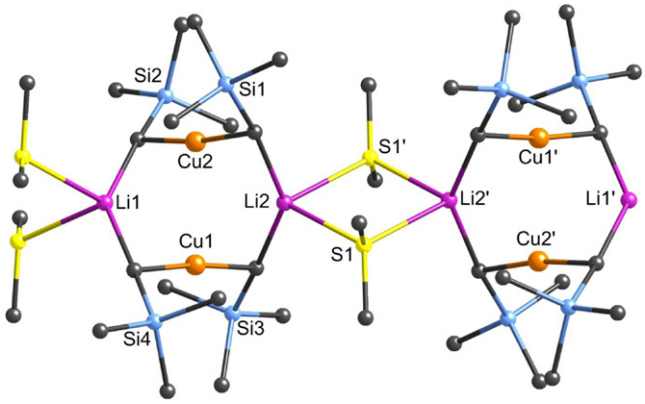

Fig. 6. Molecular structure of two repeating units of $[Cu_2Li_2(CH_2SiMe_3)_4(SMe_2)_2]_\infty$ [34].

Although the solution studies and structural characterizations discussed above all point to the dimeric form being the most prevalent and thermodynamically preferred arrangement for lithium homocuprates, the solid-state structures of two monomeric lithium diorganocuprates have also been reported (Fig. 7). In both complexes the properties of the organo group are key to favoring monomeric over dimeric aggregation. Despite their monomeric nature, the cuprate anion in both of these complexes is still directly attached to the lithium cation and they can thus be considered as contact ion pair species.

The bulky terphenyl groups in $[CuLi(C_6H_3Mes_2\text{-}2,6)_2]$ prevent the diarlycuprate from dimerising on steric grounds, and the compound exists in the solid-state as monomers [36]. There are in fact two independent monomeric lithium diarylcuprate molecules in the crystal lattice, as well as some co-crystallized copper diarylcuprate $[Cu_2(C_6H_3Mes_2\text{-}2,6)_2]$. In the first of the lithium diarylcuprate molecules the cuprate moiety is close to linear (C–Cu–C angle, 171.1(2)°) with a mean Cu–C distance of 1.940 Å. The lithium is coordinated η^1 to the *ipso*-terphenyl carbon (Li–C_{ipso}, 2.312(10) Å) and η^6 to six mesityl carbon atoms belonging to the second aryl group, mean Li–C 2.516 Å (Fig. 8). The second lithium diarylcuprate molecule possesses similar structural features to the first, with the exception that the lithium atom is now η^3 to the *ipso*-C_6H_3 carbon and an *ipso* and *ortho* mesityl carbon, and η^6 to a mesityl group of the adjacent terphenyl ligand. The η^6 interaction between the lithium and mesityl groups in both molecules is similar in nature to that observed in $[Cu_2Li_2Mes_4]$ (*vide supra*).

Solid-state characterization of the dialkylcuprate $[CuLi(CH(Me)P(Et)_2NSiMe_3)]$ also revealed a monomeric structure (Fig. 9) [37]. The cuprate unit in this complex is close to linear with a C–Cu–C bond angle of 167.2(1)° and a mean Cu–C distance of 1.954(2) Å. However, unlike the other structures discussed in this section, there are no bonding interactions between the carbanion centers and the lithium cation, and the lithium is just two coordinate to two nitrogen centers, one from each ligand, thus giving a central eight-membered cyclic motif. A related cuprate

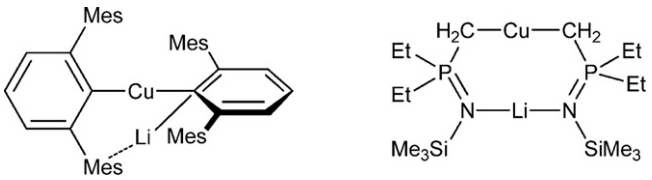

Mes = $C_6H_2Me_3$-2,4,6

Fig. 7. Crystallographically characterized monomeric lithium homo-cuprates.

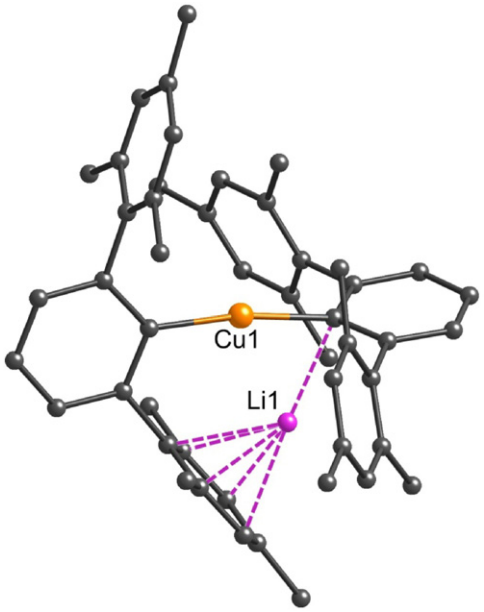

Fig. 8. Molecular structure of $[CuLi(C_6H_3Mes_2\text{-}2,6)_2]$ [36].

based on a similar organo R group has also been obtained from the reaction of $[LiCH_2P(Me)_2NSiMe_3]_4$ with copper(I) iodide and silicon grease $(-OSiMe_2-)_n$ in diethyl ether [38]. This gave crystals of $[Li(Me_3SiNP(Me)_2CH_2\text{–}Cu\text{–}CH(SiMe_2OLi)P(Me)_2NSiMe_3)]_2$ which contain lithiated silanol functionalities in addition to the lithium diorganocuprate moiety. The structure forms an overall dimeric motif, and again no carbanion–lithium interactions were observed.

Even when discounting any large steric or electronic effects caused by the ligands, theoretical calculations have suggested that monomeric homocuprates are likely to be less reactive in addition reactions than their dimeric homologs. This is because an intricate cooperation between two lithium atoms and a copper atom is thought to be required for the reaction to proceed smoothly [17,39].

2.2. Lithium diorganocuprate separated ion-pair complexes $[R_2Cu][Li]$

The lithium homo-cuprates discussed above in Section 2.1 can all be considered as contact ion pair (CIP) species, in which the lithium cation(s) remains associated with the cuprate anion(s) *via* one or more bonding interactions. Such CIP structures are usually observed when the cuprate crystals have been obtained from solutions of lithium homocuprates in either non-coordinating solvents, such as toluene or hexane, or from weakly coordinating solvents, such as ether or DMS. However, crystallization from a more polar

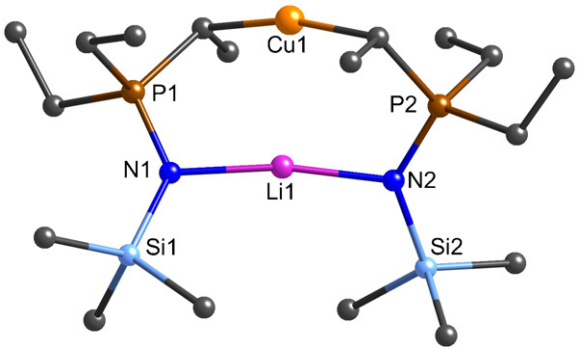

Fig. 9. Molecular structure of $[CuLi(CH(Me)P(Et)_2NSiMe_3)]$ [37].

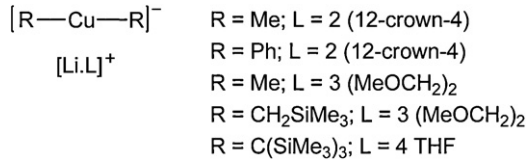

Fig. 10. Crystallographically characterized separated ion pair lithium diorganocuprates.

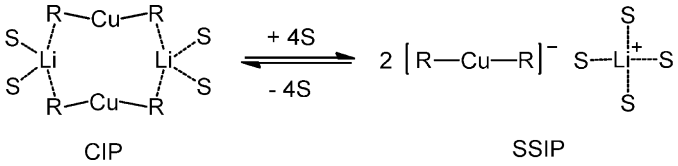

Scheme 3. The CIP–SSIP equilibrium reaction for lithium homocuprates.

solvent such as THF or DME (particularly when combined with the presence of bulky organo groups), or alternatively the addition of a strong lithium-complexing agent such as 12-crown-4, can lead to the formation of separated ion pair (SIP) structures (Fig. 10). Within these SIP species there are no significant bonding interactions observable between the solvated lithium cation and the cuprate anion.

The SIP diorganocuprate anions all display linear R–Cu–R anionic units (Fig. 11), with reported C–Cu–C angles in the range 178.5(4)–180.0(5)° [33,40,41]. The preference for this linear C–Cu–C geometry has been explained by the contribution of the copper d_z^2 orbital to the Cu–C bonds [42]. Mean bond lengths for Cu–alkyl bonds within the cuprate units are 1.934 Å (Cu–Me) [33,41], 1.937 Å (Cu–CH_2SiMe_3) [33] and 2.049 Å (Cu–$C(SiMe_3)_3$) [40]—note that the presence of partial occupancy $[Li(C(SiMe_3)_3)_2]$ anions within the crystal lattice of $[Cu(C(SiMe_3)_3)_2][Li(THF)_4]$ makes this last value less reliable. The only SIP lithium diarylcuprate to be characterized to date in the solid state is $[CuPh_2][Li(12\text{-crown-}4)_2]$ which contains Cu–C bonds of mean length 1.925 Å, slightly shorter than the comparable Cu–C distances in dialkylcuprates due to the change in hybridization of the carbon [41].

Similar R_2Cu cuprate anions have also been reported in the crystallographically characterized complexes $[Cu(dppe)_2][CuMes_2]$ [43], $[Cu(PMe_3)_4][CuMe_2]$ [44], and $[Cu(SIMes)_2][Cu(CF_3)_2]$ [45] (SIMes = 1,3-dimesitylimidazolin-2-ylidene). All of these complexes are homo-metallic and contain Cu(I) based counter-ions. $[Cu(dppe)_2][CuMes_2]$ was obtained from the addition of 1,2-bis(diphenylphosphino)ethane (dppe) to the organocopper complex Cu_5Mes_5, and comprises of a $[CuMes_2]$ linear cuprate anion (C–Cu–C angle 180.0(7)°; Cu–C 1.915(9) Å) and a tetrahedral Cu(I)-cation [43]. $[Cu(PMe_3)_4][CuMe_2]$ was formed in the reaction of anhydrous cupric acetate with dimethylmagnesium and trimethylphosphine, and contains a $[Me_2Cu]$ cuprate unit (Cu–C, 1.94(1) Å) whose linearity is imposed by crystallographic symmetry [44]. Lastly, treatment of (SIMes)Cu–O*t*Bu with Me_3SiCF_3 gave a solution of [(SIMes)Cu–CF_3] from which crystals of $[Cu(SIMes)_2][Cu(CF_3)_2]$ were grown; these crystals comprise of a linear biscarbene cationic complex of copper paired with a bis(trifluoromethyl)cuprate unit (C–Cu–C 180.0(3)°; Cu–C 1.970(6) Å) [45].

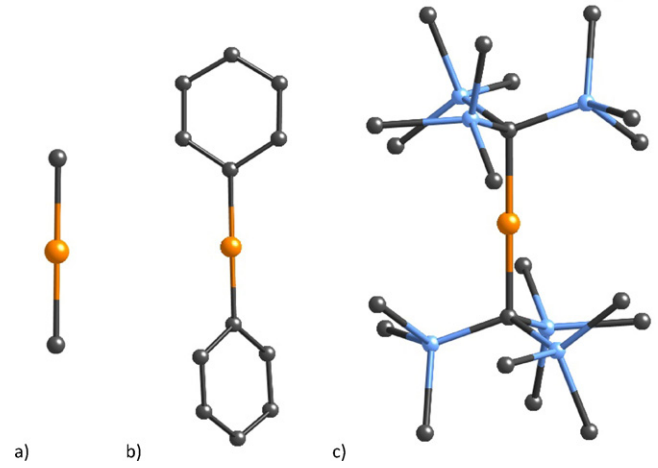

Fig. 11. Molecular structures of the diorgano-cuprate anions in (a) $[CuMe_2][Li(DME)_3]$ [33], (b) $[CuPh_2][Li(12\text{-crown-}4)_2]$ [41], and (c) $[Cu(C(SiMe_3)_3)_2][Li(THF)_4]$ [40].

The presence of lithium complexing solvents or ligands can also, not unsurprisingly, play a large role in the solution structures of lithium homocuprates, and have been shown to have a large effect on the reactivity of these species too. For example, the conjugate addition reaction of organocuprates with enones has been demonstrated to be highly dependent upon the solvent with fast conjugate addition occurring in toluene, hexane and diethylether, whilst the reaction is retarded in better coordinating solvents such as THF or pyridine [46]. In highly polar solvents such as DMF or DMSO no reaction at all was observed. Similarly, it has been reported how addition of crown ethers greatly suppress the reactivity of organocuprates [47]. These variations in homocuprate reactivity can be explained by the nature of the ion pairing in solution.

Although in the solid state the nature of the bonding is typically clear-cut, with the cuprate either crystallizing in a neutral ion paired complex or in an ion separate structure, in solution the behavior is far more dynamic with an equilibrium present between the contact ion pair (CIP) and solvent separate ion pair (SSIP) form of the cuprate (Scheme 3) [18,48]. In order to probe this equilibrium the aggregation behavior of Me_2CuLi in solution has been investigated using a series of ^1H–^6Li HOESY NMR experiments [33,49]. In these experiments the position of the CIP–SSIP equilibrium in a range of solvents was monitored by examining the intensity of the NMR cross-peak between the lithium cation and the CH_3 group of the cuprate. In diethyl ether a strong lithium–CH_3 cross peak was observed, indicating that in ether solution the main species is the CIP model. However, in THF a much weaker dipolar interaction between lithium and CH_3 was reported indicating that the equilibrium lies predominately (but not solely) on the side of the SSIP. The position of the CIP–SSIP equilibrium has also been shown to directly influence the rate of reaction of these reagents, with CIPs proving more reactive for conjugate addition reactions (thus favoring the use of diethyl ether as a solvent in these reactions), whilst SSIPs are more reactive for substitution reactions [33,50].

2.3. *Lithium diorganocuprate–lithium halide aggregates $R_2CuLi.LiX$*

Although Gilman homocuprates are often represented as R_2CuLi species or aggregates thereof (and indeed in this review so far have been considered as thus), this simple model does reflect the presence of metal salts which are usually unavoidably formed as co-products in their synthesis. Lithium diorganocuprates are most commonly prepared from the reaction of a copper(I) halide with two equivalents of an organolithium species (Scheme 2) and thus one equivalent of a lithium halide salt is also formed concomitantly with the homocuprate.

Studies on the aggregation states of organocuprates derived from copper(I) halides using electrospray ionization mass spectrometry have indicated that the lithium halide may be intimately involved in the composition of the cuprate species in solution [51].

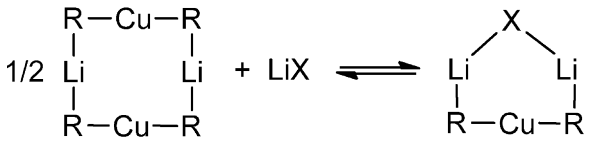

Scheme 4. Formation of lithium homocuprate–lithium halide aggregates.

The presence of LiX (X = I, Br) has also been shown to influence the reactivity of organocuprates [50,52], although it is unclear whether this is due to incorporation of the LiX moiety into a new cuprate cluster or due to some degree of stabilization of the reaction transition state afforded its presence. However, based on available NMR evidence [18,53,54] and theoretical calculations [17,39,54,55] a model for the formation of a mixed homocuprate–lithium halide aggregate in solution has been proposed comprising of a closed cluster in which two lithium cations remain associated with the cuprate anion (Scheme 4).

Although the majority of lithium homocuprates characterized in the solid state to date have been prepared from solution reaction mixtures of copper(I) halides and organolithiums (the other main route being the direct reaction of an organocopper with an organolithium reagent), there is no evidence of any LiX incorporation into the resultant solid-state structures. The only exception to this is the series of related compounds $[Cu(C_6H_4(CH_2N(Et)CH_2CH_2NEt_2)\text{-}2)_2Li_2Br]$ [56], $[Cu(C_6H_4(CH_2N(Me)CH_2CH_2NMe_2)\text{-}2)_2Li_2Br]$ [57], and $[Cu(1\text{-}C_{12}H_8(CH_2N(Me)CH_2CH_2NMe_2)\text{-}2)_2Li_2Br]$ [57] (Fig. 12).

$[Cu(C_6H_4(CH_2N(Et)CH_2CH_2NEt_2)\text{-}2)_2Li_2Br]$ was prepared from reaction of two molar equivalents of the diamine chelated aryllithium $[Li(C_6H_4(CH_2N(Et)CH_2CH_2NEt_2)\text{-}2)]_2$ with copper(I) bromide (Fig. 13) [56]. The aryl R groups bridge the copper and lithium centers in an analogous fashion to that observed in lithium homocuprate dimers (Section 2.1). Mean Li–C_{ipso} and Cu–C_{ipso} distances are 1.931(4) and 1.941(4) Å respectively, with a C–Cu–C bond angle of 165.13(15)°. The structure can be considered as a contact ion pair comprising of two ionic fragments, a $[R_2Cu]^-$ cuprate anion and a $[Li–Br–Li]^+$ cation, held together both by electrostatic Li–C_{ipso} interactions and by chelation of the lithiums by the *ortho*-amine substituents on the aryl R group. The introduction of these donor amine groups is thought to play a large role in contributing to the thermodynamic stability of this complex. Within the crystal structure, the lithium sites are partly occupied by copper atoms (refined occupancies of up to 9% Cu) indicating that corresponding Cu_2Li and Cu_3 complexes are isomorphous. Moreover, the homologous $[Cu_3R_2Br]$ aryl copper–copper bromide aggregate has also been structurally characterized [58], lending credence to this assertion.

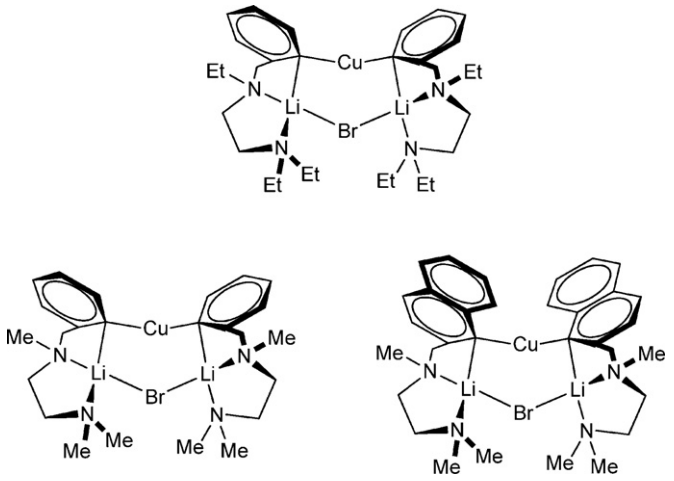

Fig. 12. Crystallographically characterized $CuLiR_2$.LiX complexes.

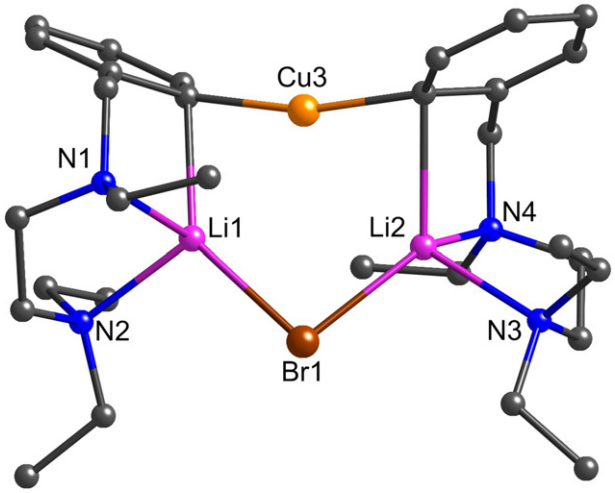

Fig. 13. Molecular structure of $[Cu(C_6H_4(CH_2N(Et)CH_2CH_2NEt_2)\text{-}2)_2Li_2Br]$ [56].

It is interesting to note that benzylic nitrogen centers in $[Cu(C_6H_4(CH_2N(Et)CH_2CH_2NEt_2)\text{-}2)_2Li_2Br]$ become stereogenic upon Li-coordination, but within the crystal structure and also in solution (as determined using ^1H NMR experiments) only RR and SS enantiomeric isomer pairs are observed, with the RS and SR stereoisomer pair absent. The other two crystallographically characterized $R_2CuLi.LiX$ aggregate complexes, $[Cu(C_6H_4(CH_2N(Me)CH_2CH_2NMe_2)\text{-}2)_2Li_2Br]$ and $[Cu(1\text{-}C_{12}H_8(CH_2N(Me)CH_2CH_2NMe_2)\text{-}2)_2Li_2Br]$, also exhibit very similar solid-state structures to $[Cu(C_6H_4CH_2NEtCH_2CH_2NEt_2\text{-}2)_2Li_2Br]$ and show similar behavior in solution [57]. This is perhaps not surprising given all contain similar diamine *ortho*-substituted aryl groups.

2.4. Copper-rich lithium homocuprates $R_{n+m}Cu_nLi_m$ ($n > m$)

When Gilman reported the first synthesis of a lithium organocuprate (Scheme 2), he described how addition of one equivalent of organolithium to copper(I) iodide gave a precipitate of organocopper CuR which dissolved on addition of another equivalent of organolithium to give the lithium homocuprate "$LiCuR_2$". However, subsequent studies went on to show that the addition of less than a full equivalent of organolithium to the organocopper precipitate could also, in some cases, result in the precipitate redissolving. This led to speculation that copper-rich lithium cuprate aggregates, $R_{n+m}Cu_nLi_m$ ($n > m$), were being formed in solution.

Attempts to characterize these copper-rich lithium organocuprates initially employed ^1H NMR spectroscopy to study the species formed during the treatment of methylcopper with less than one equivalent of methyllithium. When the reaction solvent was THF or dimethyl ether the results were interpreted to show the presence of $LiCu_2Me_3$ species, whereas in diethyl ether $Li_2Cu_3Me_5$ species were inferred [52,59,60]. Further studies on the reactivity of the supposed $Li_2Cu_3Me_5$ species suggested a new type of aggregate was formed which was far superior to Me_2CuLi for conjugate methylation of enals [61]. A number of copper-rich lithium homocuprate aggregates have subsequently been isolated and characterized in the solid state (Fig. 14).

The very first organocuprate to be crystallographically characterized was the anionic pentanuclear copper cluster $[Cu_5Ph_6]^-$ which was crystallised as its $[Li(THF)_4]^+$ and $[Li(PMDETA)(THF)]^+$ salts (PMDETA = *N*,*N*′,*N*″,*N*‴-pentamethyldiethylenetriamine) from the reaction of copper(I) bromide with two equivalents of phenyllithium [62]. The overall Li:Cu ratio in this cuprate is therefore 1:5.

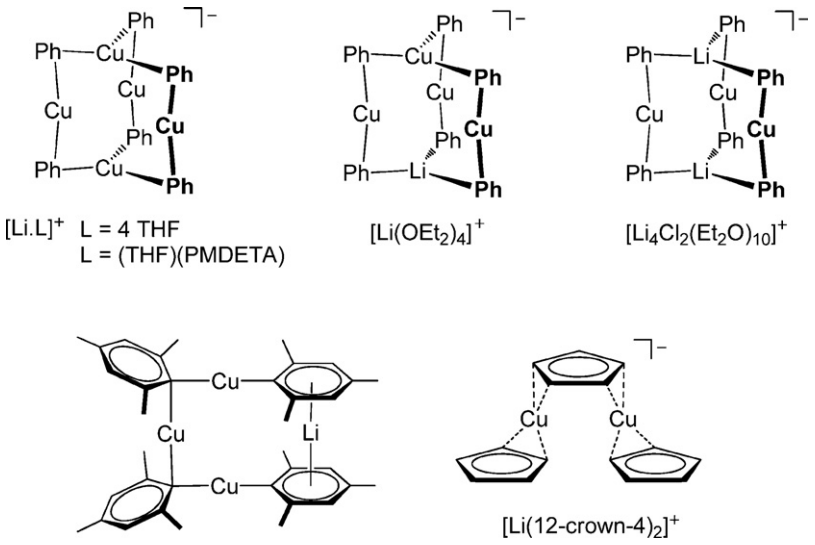

Fig. 14. Crystallographically characterized copper-rich lithium homocuprates.

The mono-anionic $[Cu_5Ph_6]^-$ cluster adopts a somewhat flattened trigonal bipyramidal structure comprising of five copper atoms, three in equatorial and two in axial positions, with six phenyl groups bridging the axial–equatorial edges (Fig. 15a). It can best be considered as three $[CuPh_2]^-$ units, each based on an equatorial copper, bridged by two axial copper cations. The three equatorial coppers are approximately linearly coordinated with an average C–Cu_{eq}–C bond angle of 167(1)° and Cu–C_{eq} distance of

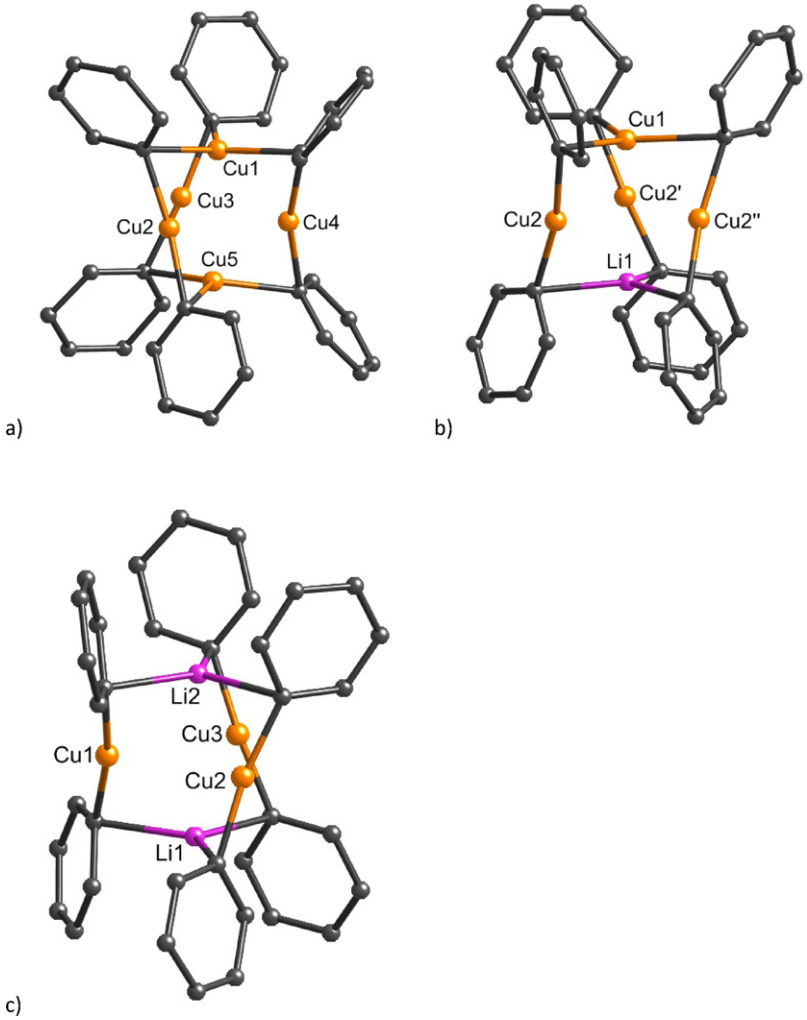

Fig. 15. Molecular structures of the cuprate anions in (a) $[Cu_5Ph_6][Li(thf)_4]$ [62], (b) $[Cu_4LiPh_6][Li(OEt_2)_4]$ [63], and (c) $[Cu_3Li_2Ph_6]_2[Li_4Cl_2(OEt_2)_{10}]$ [64].

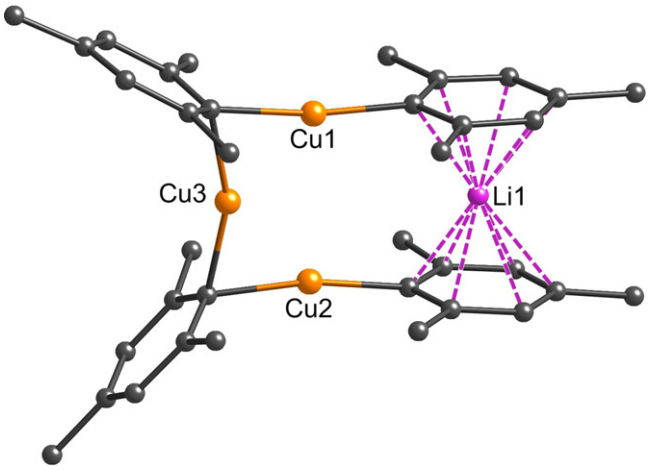

Fig. 16. Molecular structure of $[Cu_3LiMes_4]$ [31].

1.98(1) Å. In contrast the axial coppers adopt approximately trigonal planar geometries with more elongated C–Cu_{ax} bond distances (mean, 2.17(2) Å) [62].

Shortly afterwards the solid-state structures of $[Cu_4LiPh_6][Li(OEt_2)_4]$ [63] and $[Cu_3Li_2Ph_6]_2[Li_4Cl_2(OEt_2)_{10}]$ [64] were reported. In these structures one or two of the axial copper cations respectively have been formally replaced by lithium cations. Each cluster adopts a similar trigonal bipyramidal penta-metallic motif.

$[Cu_4LiPh_6][Li(OEt_2)_4]$ (Fig. 15b) was isolated from the reaction of copper(I) bromide and phenyllithium in diethyl ether, using almost identical reaction conditions to those employed in the preparation of the pentacopper cluster above [63]. The axial lithium site is contaminated with a significant amount of copper (refined occupancy of 89% Li, 11% Cu). Within the anion the bonding distances and geometries are similar to those observed in $[Cu_5Ph_6]^-$: mean Cu_{eq}–C and Cu_{ax}–C distances are 1.96(4) and 2.33(3) Å respectively, Li–C distances are 2.16(4) Å, and the equatorial coppers are near to linear in geometry (C–Cu_{eq}–C, 168.1(18)°). A closely analogous magnesium organocuprate complex $[Cu_4MgPh_6]$, was also reported in the same paper, and its structure is discussed further in Section 4.

$[Cu_3Li_2Ph_6]_2[Li_4Cl_2(OEt_2)_{10}]$ (Fig. 15c) was isolated from the reaction of copper(I) cyanide and two equivalents of phenyllithium in diethyl ether, with the surprising presence of chloride anions in the structure being attributed to contamination of the copper cyanide starting material [64]. Unlike the other organocuprates in this section, $[Cu_3Li_2Ph_6]_2[Li_4Cl_2(OEt_2)_{10}]$ is not actually a copper-rich species, but rather a lithium homocuprate–lithium halide aggregate of stoichiometry $LiCuPh_2 \cdot 1/3LiCl$. However it merits inclusion in this section due to the structural parallels it exhibits with the previously discussed $[Cu_5Ph_6]^-$ and $[Cu_4LiPh_6]^-$ anions. The $[Cu_3Li_2Ph_6]^-$ anion is more axially elongated and therefore less squashed that the $[Cu_5Ph_6]^-$ anion, however the Cu–C distances are comparable, mean 1.929(6) Å. The C–Cu–C angles in the cuprate units are at 169.03° (av.) close to linear, and the typical Li–C distance is 2.240(14) Å. The homologous silver complex $[Li_2Ag_3Ph_6]_2[Li_4Br_2(OEt_2)_{10}]$ has also been isolated and structurally characterized [65].

More recently the 3:1 Cu:Li cuprate $[Cu_3LiMes_4]$ was isolated from the reaction of mesityl copper with mesityl lithium [31]. The X-ray crystal structure contains two independent but structurally similar $[Cu_3LiMes_4]$ cuprate molecules (one of which is shown in Fig. 16). These tetranuclear complexes can be considered as either a dimer similar to $[Cu_2Li_2Mes_4]$ (see Section 2.1) with one the lithium cations replaced by a copper center, or alternatively as a

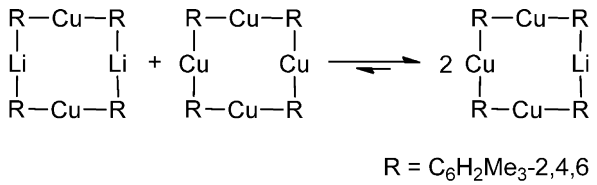

Scheme 5. Interaggregate metal exchange in lithium mesitylcuprates [31].

$[Cu_4Mes_4]$ tetramer with one of the copper atoms replaced by a lithium. The lithium cation in $[Cu_3LiMes_4]$ is sandwiched directly between two aromatic rings with η^6,η^6 coordination (mean C–Li, 2.393(8) Å). The Mes_2Cu_3 'half' of the complex is similar in structure to that of $[Cu_4Mes_4]$ [66] with the mesityl groups arranged approximately orthogonal to the Cu–Cu axes and coordinated to two copper centers *via* their *ipso*-carbon to give 3 center–2 electron Cu–C–Cu bonds. The average Cu–C distance within these bonds is 2.007(4) Å; this is comparable with Cu–C bond distances in $[Cu_4Mes_4]$ (mean 1.993(10) Å) [66]. The remaining Cu–C bonds are all shorter (mean 1.936(4) Å), and therefore similar in length to the Cu–C bonds in $[Cu_2Li_2Mes_4]$ (av. 1.930(2) Å) [31]. They can likewise be considered as 2 center–2 electron σ-bonds.

It had been previously postulated that such Cu_3LiR_4 species could also be present in lithium diarylcuprate solutions due to interaggregate exchange between $Cu_2Li_2R_4$ and Cu_4R_4 molecules [67,68]. In agreement with this hypothesis, reaction of $[Cu_2Li_2Mes_4]$ with $[Cu_4Mes_4]$ in benzene (monitored *in situ* using ^{7}Li NMR spectroscopy) was observed to result in the exclusive formation of $[Cu_3LiMes_4]$. The reaction sat far on the side of the 3:1 Cu:Li species with no evidence of formation of the 2:2 and 4:0 species from the back reaction (Scheme 5) [31].

The only other copper rich lithium homocuprate to have been structurally characterized is the separated ion pair complex $[Cp_3Cu_2][Li(12\text{-crown-}4)_2]$ (Cp = cyclopentadienyl) formed in the reaction of copper(I) chloride with two equivalents of cyclopentadienyl lithium in the presence of 12-crown-4 [69]. The structure contains an overall 2:1 copper to lithium ratio due to the presence of a $[R_3Cu_2]^-$ cuprate anion and a 12-crown-4 solvated lithium cation. The cyclopentadienyl ligands in this complex adopt an η^2 coordination motif to the copper centers [69].

2.5. *Higher-order lithium homocuprates $R_{n+m}Cu_nLi_m$ (n < m)*

Organocuprates in which the ratio of organo group to copper is greater than 2:1 and in addition the copper center is bound to three or more organo groups, for example to give $[CuR_3]^{2-}$ or $[CuR_4]^{3-}$ units, are often termed "higher order". This therefore differentiates them from "lower-order" or Gilman-type organocuprates R_2CuLi where the R:Cu ratio is exactly 2:1 and the linear copper centers are bound to just two organo groups yielding mono-anionic $[R_2Cu]^-$ units (see Sections 2.1 and 2.2). The existence and composition of these so-called higher-order species has proven somewhat controversial over the years.

Higher-order organocuprates are typically prepared from the addition of more than two equivalents of an organolithium to a copper(I) salt. The reactivity of these reagents has been studied for a range of organic synthetic transformations, and they have been purported to exhibit enhanced reactivity over lower order organocuprates in many situations, for example in S_N2 reactions [9,70]. Purported higher-order cuprates derived from copper(I) cyanide have attracted particular attention in the literature. However, due to their unique spectroscopic properties and reactivity, cyanocuprates are often considered as a distinct class of reagent in their own right, and thus are considered separately in Section 3.

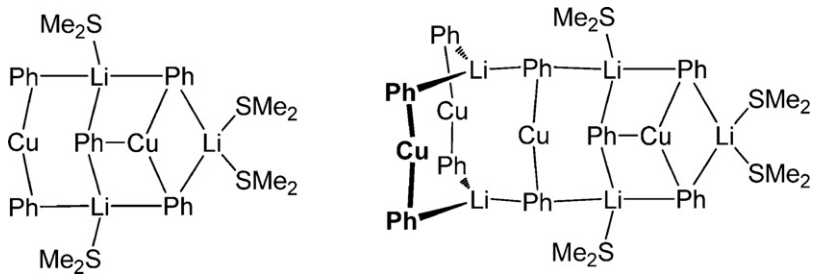

Fig. 17. Crystallographically characterized higher-order lithium arylcuprates.

Studies probing the solution composition of higher-order organocuprates have often proven inconsistent and are also very dependent upon the solvent system employed. However, the existence of both R_3CuLi_2 and $R_5Cu_2Li_3$ cluster species has been inferred. Mixtures of methyllithium and methylcopper were first postulated to give Li_2CuMe_3 aggregates when the methyllithium was in twofold excess based on the results of a series of NMR studies in Me_2O, Et_2O and THF [52,59,60]. In addition, these Me_3CuLi_2 species were shown to exist in an equilibrium reaction with MeLi and their lower-order Me_2CuLi organocuprate derivative. However, later ^{13}C NMR studies on isotopically enriched $Li_2Cu(^{13}CH_3)_3$ species suggested that the predominate THF solution structure is in fact lower order in nature, and that the lithium atoms remain only very weakly associated and likely spend a substantial amount of time dissociated from the anionic core [71]. Moreover, a ^{13}C and ^{6}Li NMR study on Ph_3CuLi_2 in diethyl ether and THF revealed only a mixture of PhLi and Ph_2CuLi to be present [53]. However, in dimethyl sulfide a discrete Ph_3CuLi_2 species was identified. Further studies on mixtures of phenyllithium and copper(I) bromide in dimethyl sulfide led to the isolation and structural characterization of two higher-order arylcuprate complexes (Fig. 17) [28,72].

The cuprate $[Cu_2Li_3Ph_5(SMe_2)_4]$ was crystallized from a reaction mixture comprising of three equivalents of phenyllithium and one of copper(I) bromide in dimethyl sulfide after the removal of the LiBr by-product [72]. There are two chemically identical but crystallographically independent molecules within the crystal lattice, one of which is shown in Fig. 18. The structure can be considered to consist of one lower-order $[Ph_2Cu]^-$ cuprate unit and one higher-order $[Ph_3Cu]^{2-}$ cuprate unit. These two units are linked together by means of three bridging lithium cations. Four lithium-coordinating Me_2S molecules are also present. The overall Ph:Cu ratio within the structure is therefore 2.5:1. Within the $[Ph_2Cu]^-$ moiety the average C_{ipso}–Cu distance is 1.93 Å and the C–Cu–C angle is 164.6(2)°. These parameters are similar to those reported for other diphenyl cuprate units in lower-order organocuprates such as $[Ph_4Cu_2Li_2(OEt_2)_2]$ [27] $[Ph_2Cu][Li(12\text{-crown-}4)_2]$ [41], and $[Cu_3Li_2Ph_6][Li_4Cl_2(OEt_2)_{10}]$ [64]. In comparison, the copper atom within the higher-order $[Ph_3Cu]^{2-}$ moiety is close to trigonal planar in geometry (sum of angles about copper, 357.1°) and the Cu–C_{ipso} distances are longer (average 2.02 Å) owing to the higher coordination number of the copper. Variable temperature ^{13}C NMR studies have confirmed that $[Cu_2Li_3Ph_5]$ retains its higher-order structure in dimethyl sulfide solution [73].

The closely related complex $[Cu_4Li_5Ph_9(SMe_2)_4]$ was prepared from the addition of 3.3 equivalents of phenyllithium to copper(I) bromide in dimethyl sulfide, again after removal of the LiBr by-product [28]. The solid-state structure contains three $[Ph_2Cu]^-$ units and one $[Ph_3Cu]^{2-}$ unit, giving an overall Ph:Cu ratio of 2.25:1 (Fig. 19). It is interesting to note that this ratio is lower than that observed for $[Cu_2Li_3Ph_5(SMe_2)_4]$ despite the application of an extra 0.3 equivalents of phenyllithium. The three linear, lower-order cuprate units are triply bridged by lithium cations to give a $[Li_2Cu_3Ph_6]^-$ moiety, structurally similar to the anion in $[Cu_3Li_2Ph_6][Li_4Cl_2(OEt_2)_{10}]$ [64] (see Section 2.4). This then associates with the higher-order trigonal cuprate unit, three additional lithium cations and four DMS molecules to give the aggregate species observed in the crystal structure. Bond distances within the $[Ph_2Cu]^-$ units, average 1.93 Å, are shorter than those observed in the $[Ph_3Cu]^{2-}$ unit, average 2.02 Å.

A higher-order lithium alkynyl cuprate has also been isolated from the reaction of copper(I) bromide and phenylethynyl-

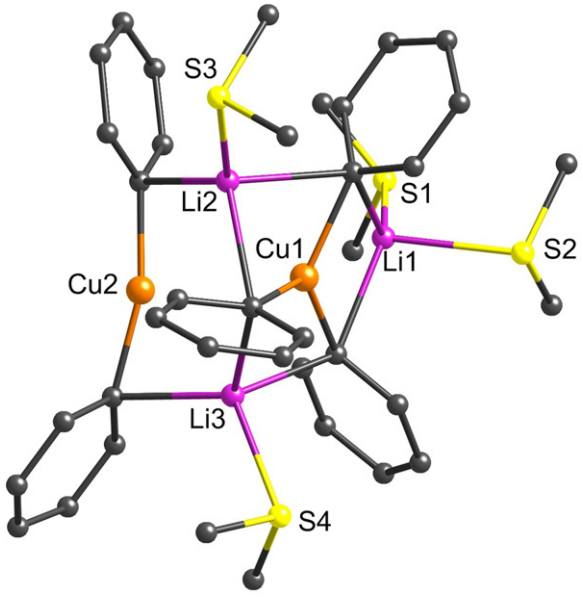

Fig. 18. Molecular structure of $[Cu_2Li_3Ph_5(SMe_2)_4]$ [72].

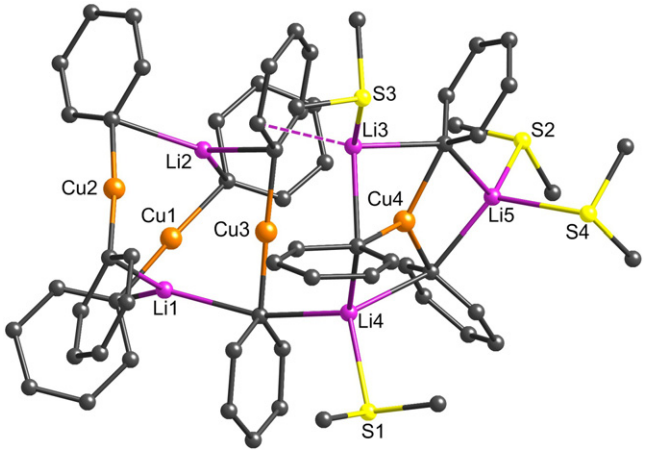

Fig. 19. Molecular structure of $[Cu_4Li_5Ph_9(SMe_2)_4]$ [28].

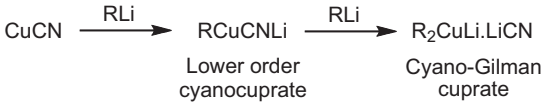

Scheme 6. The preparation of lower order cyanocuprates and cyano-Gilman (Lipshutz) reagents.

lithium in diethyl ether. Solid-state structural characterization revealed a large aggregated cluster $[(PhC{\equiv}C)_{10}Cu_4Li_6(OEt_2)_3]$ with a PhC≡C:Cu ratio of 2.5:1 [74]. The structure exhibits some significant differences to the higher-order aryl cuprates discussed above, and is perhaps best considered as comprising of three lower-order $[(PhC{\equiv}C)_2Cu]^-$ cuprate units and one higher-order $[(PhC{\equiv}C)_4Cu]^{3-}$ cuprate unit aggregated together with six lithium cations and three diethyl ether molecules. Within the unique, formally trianionic $[(PhC{\equiv}C)_4Cu]^{3-}$ cuprate moiety the copper center is tetrahedrally surrounded by the four alkynyl ligands (C–Cu–C in range 108–111°; Cu–C in range 1.97–2.02 Å). In contrast, the two coordinate copper centers in the $[(PhC{\equiv}C)_2Cu]^-$ units are close to linear (C–Cu–C, 170–173°) and the Cu–C bonds are, at 1.83–1.89 Å, significantly shorter.

3. Lithium cyanocuprates

Cyanocuprates can be formed from the reaction of either one or two equivalents of organolithium reagent (RLi) with copper(I) cyanide, thus giving compounds of stoichiometry RCu(CN)Li and $R_2Cu(CN)Li_2$ respectively (Scheme 6). The term "higher order" was introduced for the later of these species by Lipshutz [70], and these reagents are also sometimes referred to as Lipshutz or cyano-Gilman cuprates in the literature.

The reactivity and stability of cyanocuprates, and in particular Lipshutz cuprates, have been shown to differ (considerably in some cases) from homocuprates derived from copper(I) halides, *i.e.*, Gilman homocuprates of stoichiometry R_2CuLi or $R_2CuLi.LiBr/I$. This has led to cyanocuprates being considered as a distinct class of cuprate reagent in their own right, and there have been many studies published concerning their specific synthetic applications [75].

3.1. Lower-order lithium cyanocuprates RCuCNLi

The first reports on lower-order cyanocuprates (as they were later to become known) involved the treatment of an alkyl lithium with one equivalent of copper(I) cyanide to give a new "unsymmetrical reagent" [76]. These reagents were shown to be useful in performing 1,4-addition reactions with enones, as well as in displacing halide ions from alkyl halides, and in some cases exhibited yields higher that those obtained with "symmetrical" R_2CuLi Gilman-type reagents. The structures for these new cyanocuprate reagents were predicted to be of the form $[RCu(CN)]^-Li^+$ in which one alkyl and one cyano group were coordinated to the same copper center. This structural motif was later confirmed in solution using ^{13}C NMR on the isotopically labeled cyanocuprate $EtCu(^{13}CN)Li$. Observation of a direct coupling between the cyano and ethyl carbanion centers confirmed that both were directly connected to the same copper center [77]. This structural motif has also been corroborated by a number of solid-state characterizations (Fig. 20).

The solid-state characterizations of lower-order cyanocuprates all show the presence of linear $[R–Cu–CN]^-$ heteroleptic cuprate units. These cuprate units tend to undergo dimerization by way of the cyano nitrogen atom and the lithium cation, thus giving rise to a four-membered N_2Li_2 ring. This is exemplified by the X-ray structures of the THF adducts $[RCu(CN)Li(THF)_2]_2$ where $R = C_6H_3(Trip)_2$-2,6 (Trip = $C_6H_2iPr_3$-2,4,6) [78], $C(SiMe_3)_3$ [79], $C(SiMe_3)_2(SiMe_2NMe_2)$ [79], or $C(SiMe_2Ph)_3$ [80], and also in the diethyl ether adducts $[RCuCNLi(OEt_2)_2]_2$ where $R = Me_3SiCH_2$ [81] or *t*Bu [82]. This type of dimerization is therefore very different from the dimerization mode observed in Gilman homocuprates (see Section 2.1). The solid-state structure of $[(C_6H_3Trip_2$-2,6)$CuCNLi(THF)_2]_2$ is shown in Fig. 21 as a representative example of a lower-order cyanocuprate [78]. The two-coordinate copper centers in the structure are close to linear (C–Cu–CN, 175.6(2)°) and the Cu–C(organo) distance, 1.906(4) Å, is generally shorter than analogous Cu–C distances in homocuprates. The Cu–CN distance, 1.858(5) Å, is much shorter than the Cu–C(organo) distance as is to be expected due to the sp hybridization of the cyano carbon atom and also the small size of the cyano group. The two lithium cations adopt distorted tetrahedral geometries and are each coordinate to two THF oxygen atoms (mean Li–O 1.93(1) Å) and two cyano nitrogens (mean Li–N, 2.05(1) Å).

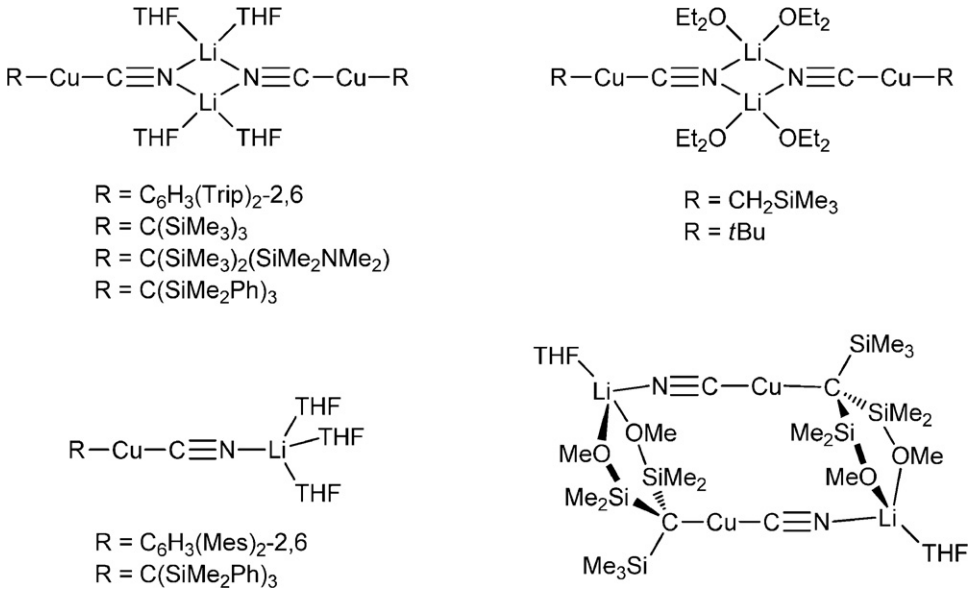

Fig. 20. Crystallographically characterized lower-order lithium cyanocuprates.

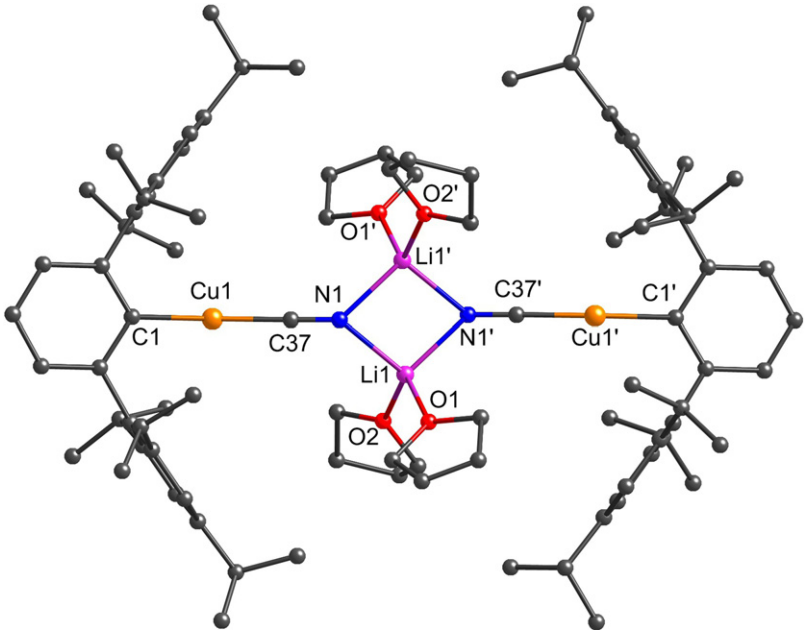

Fig. 21. Molecular structure of $[(C_6H_3Trip_2\text{-}2,6)CuCNLi(THF)_2]_2$ [78].

The solid-state structure of $[t\text{BuCuCNLi}(OEt_2)_2]_2$ is particularly intriguing as there are close contacts between the copper centers of neighboring dimeric units, Cu···Cu = 2.713(1) Å [82]. These short Cu···Cu distances, combined with the perceived bending of the cuprate units towards one another at the copper centers, were interpreted to indicate the presence of $Cu(d^{10})$–$Cu(d^{10})$ bonding. Taking into account these metal–metal interactions, the cyancuprate dimers can be considered to aggregate into polymeric chains to give $[t\text{BuCuCNLi}(OEt_2)_2]_\infty$ (Fig. 22). The nature of $Cu(d^{10})$–$Cu(d^{10})$ bonding in solid-state structures such as $[t\text{BuCuCNLi}(OEt_2)_2]_\infty$ has been a topic of much debate, and recent computational studies have suggested that such interactions are likely to be very weak in nature and mainly dependent upon the presence of other supramolecular interactions within the crystal lattice [83].

Cryoscopic molecular mass measurements have demonstrated the presence of monomeric as well as dimeric forms of lower-order cyanocuprates in THF solutions [84]. In addition, two monomeric cyanocuprates have also been structurally characterized, namely $[(C_6H_3Mes_2\text{-}2,6)CuCNLi(THF)_3]$ [85] and $[(Me_2PhSi)_3CCuCNLi(THF)_3]$ [80]. Both are contact ion pair structures in which the lithium cation is associated to the cuprate unit by coordination to the cyano nitrogen atom. The coordination sphere of the lithium is completed by three THF oxygens, giving an overall tetrahedral geometry at lithium. The C(organo)–Cu–C≡N–Li atoms within these structures adopt a linear arrangement.

The lower-order cyanocuprate $[(Me_3Si)(Me_2(MeO)Si)_2CCuCNLi(THF)]_2$ has been observed to adopt a different kind of dimeric structure [79]. In contrast to previously discussed cyanocuprate dimers, instead of forming a N_2Li_2 dimerization motif at the cyano groups the two linear C(organo)–Cu–C≡N–Li units lie antiparallel to one another are held together by coordination of the lithium cations by two methoxy groups from the neighboring unit.

3.2. Cyano-Gilman (Lipshutz) cuprates $R_2CuLi.LiCN$

Cyano-Gilman or Lipshutz cuprates can be formed from the reaction of copper(I) cyanide with two equivalents of organolithium reagent (Scheme 6), and have found a significant role in organic synthesis where they have been reported to show special reactivity in Michael addition and nucleophilic substitution reactions [9,10,70,75]. In order to explain the difference in reactivity and stability between Lipshutz cuprates and traditional Gilman-type $R_2CuLi(.LiX)$ homocuprates several different structural models have been proposed. The key to understanding these species was thought to be the location of the cyano-group, and whether it is bound to the copper center to give a true higher order $[R_2Cu(CN)]^{2-}$ dianionic cuprate unit, or whether the cyano group remains distant

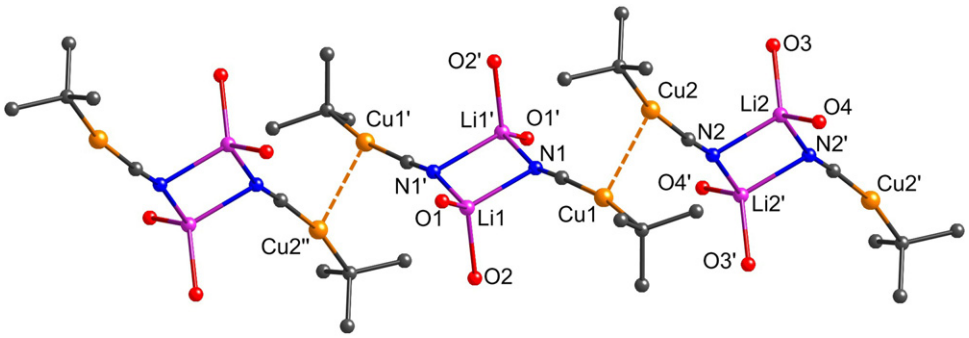

Fig. 22. Molecular structure of three repeating units of $[t\text{BuCuCNLi}(OEt_2)_2]_\infty$. Ethyl groups omitted for clarity [82].

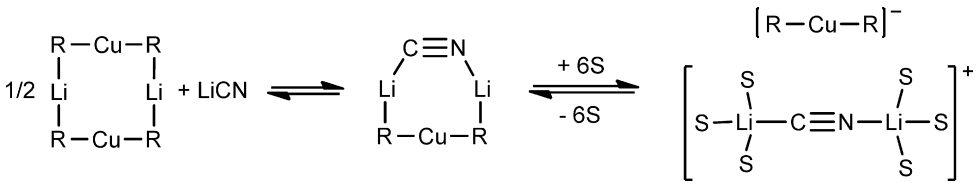

Scheme 7. Solution behavior of cyano-Gilman (Lipshutz) reagents.

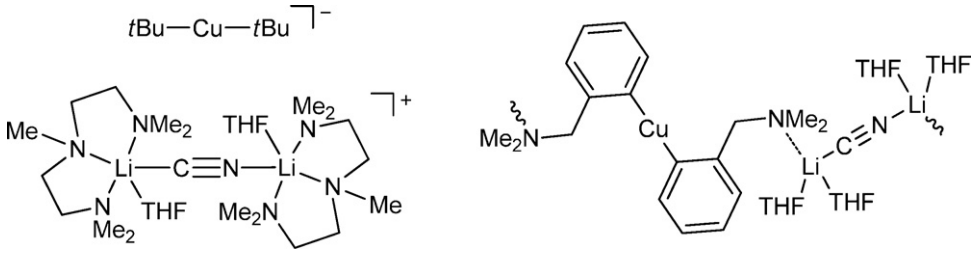

Fig. 23. Crystallographically characterized cyano-Gilman cuprates.

from the copper center resulting in distinct mono-anionic $[R_2Cu]^-$ cuprate units in a $R_2CuLi.LiCN$ cyano-Gilman type structure. There have been many heated discussions in the literature as to which of these models was most likely to be correct, with many of the early studies presenting contradictory evidence. However, the second of these representations based on homoleptic $[R_2Cu]^-$ cuprate units is now commonly accepted to be the correct representation [86].

Evidence for the formation of cyano-Gilman type structures containing $[R_2Cu]^-$ anions came from several different sources. Primarily ^{13}C NMR spectroscopic studies on cyanocuprates prepared from $Cu^{13}CN$ and two equivalents of alkyllithium showed no coupling between the alkyl group and the cyanide ligand, thus indicating both were unlikely to be bound to the same copper atom. In addition, the absence of any Cu–CN bonding was also noted for $Bu_2Cu(CN)Li_2$ in THF solution using EXAFS (Extended X-ray absorption fine structure) and XANES (X-ray absorption near edge structure) studies [87,88]. Subsequent infra-red [89], NMR [71,90], and cryoscopic [84] studies along with theoretical calculations [91–93] all suggested a $R_2CuLi.LiCN$ cyano-Gilman type structure.

Similar to traditional lithium homocuprate reagents, the structures of cyano-Gilman cuprates have been shown to be highly solvent dependent with contact ion pair (CIP) species favored in diethyl ether and solvent separated ion pairs (SSIPs) favored in THF (Scheme 7) [33,48,49]. In addition, with behavior that closely parallels that of lithium homocuprate–lithium halide aggregates (see Section 2.3), cyano-Gilman reagents have been shown to exist in an equilibrium in diethyl ether between their heterodimer (R_2CuLi_2CN) and homodimer ($R_4Cu_2Li_2$) forms, with a significant contribution from the latter [94,95].

Additional evidence for the most thermodynamically stable structural motif in "higher-order" cyanocuprates came from the solid-state characterizations of two complexes: $[tBu_2Cu][Li_2(CN)(PMDETA)_2(THF)_2]$ (PMDETA = *N*,*N*′,*N*′,*N*″,*N*″-pentamethyldiethylenediamine) [82] and $[(C_6H_4(CH_2NMe_2)\text{-}2)_2CuLi_2(CN)(THF)_4]_\infty$ [96] (Fig. 23). Both structures exhibit the same key structural features, namely a two coordinate-copper center in a linear arrangement akin to the diorganocuprate units observed in Gilman reagents, and in addition a $[Li–CN–Li]^+$ cationic moiety.

The structural determination of $[tBu_2Cu][Li_2(CN)(PMDETA)_2(THF)_2]$ shows the reagent to exist in the solid-state as a separated ion pair complex (Fig. 24) [82]. The $[tBu_2Cu]^-$ cuprate anion is linear at copper (C–Cu–C, 180.0°) with Cu–C distances of 1.957(4) Å. The cuprate unit is therefore directly analogous to $[R_2Cu]^-$ anions observed in ion-separated lithium homocuprates (Section 2.2). The four atoms in the $[Li–C\equiv N–Li]^+$ cation lie on a close to linear trajectory, with each lithium additionally surrounded by a THF oxygen atom and three nitrogen atoms from the PMDETA ligand. It was not possible to crystallographically differentiate the carbon and nitrogen atoms of the cyanide group in the structure, and the Li–C/N(cyano) bond distance was reported as 2.105(7) Å.

The solid-state structure of the cyano-Gilman cuprate $[(C_6H_4(CH_2NMe_2)\text{-}2)_2CuLi_2(CN)(THF)_4]_\infty$ also shows the presence of $[R_2Cu]^-$ cuprate anions (C–Cu–C, 180.0°; Cu–C_{ipso} = 1.917(2) Å)

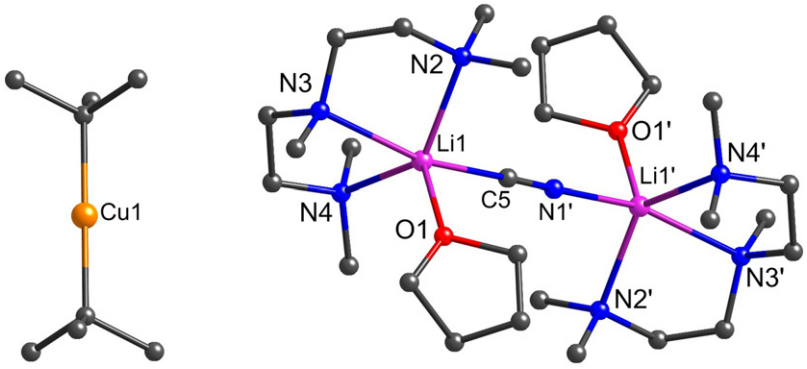

Fig. 24. Molecular structure of $[tBu_2Cu][Li_2(CN)(PMDETA)_2(THF)_2]$ [82].

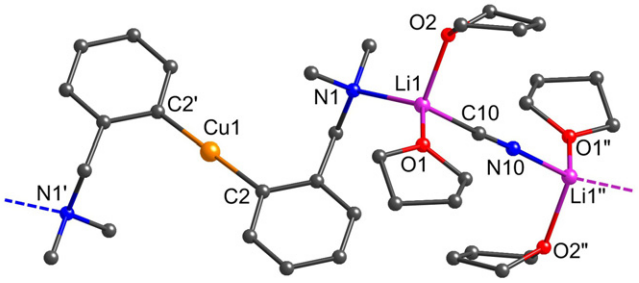

Fig. 25. Molecular structure of one repeating unit in $[(C_6H_4(CH_2NMe_2)\text{-}2)_2CuLi_2(CN)(THF)_4]_\infty$ [96].

[86]. However in this case, coordination of the lithium atom by a dimethylamino group from an adjacent cuprate unit (Li–N, 2.090 Å) results in formation of a linear zig-zag chain of alternating $[R_2Cu]^-$ anionic and $[Li_2(CN)(THF)_4]^+$ cationic units (Fig. 25). The lithium cations are further coordinated by two molecules of THF rendering each lithium four coordinate.

Despite these breakthroughs in our understanding of the structures of "higher-order" cyanocuprates and their recognition now as cyano-Gilman $R_2CuLi.LiCN$ type reagents, the reasons behind their purported high reactivity and stability remain somewhat elusive. Moreover, kinetic studies comparing the reactivity of iodo-Gilman ($R_2CuLi.LiI$) and cyano-Gilman ($R_2CuLi.LiCN$) reagents have even called these professed reactivity differences into question (at least in Michael addition reactions to 2-cyclohexenone) [50]. However, some degree of increased reactivity for cyano-Gilman over iodo-Gilman reagents is unequivocal, whatever its magnitude, and these cyano species therefore still remain reagents of choice for many organic transformations.

Several theories have subsequently been put forward to explain the origin of the higher reactivity of cyanocuprates. It has been suggested that other minor structural isomers containing heteroleptic $[RCuCN]^-$ type units (or even true higher-order $[R_2CuCN]^{2-}$ units) might also be present in solution, and which despite their low equilibrium concentration could be kinetically active and therefore play a large role in the reactivity of these systems [86,88,97]. There is, however, currently little experimental evidence for the existence of any such equilibrium reactions occurring. Alternatively, theoretical calculations have shown that the higher Lewis acidity of the $[LiCNLi]^+$ group as well as its ability to energetically stabilize the transition state in some situations, could result in higher reactivity for cyanocuprate reagents [17,97]. On the other hand, recent studies concerning the aggregation states of organocuprate species in solution have indicated that alkyl cyanocuprates ($R_2CuLi.LiCN$, R = Me, CH_2SiMe_3) show significantly higher aggregation levels (beyond dimeric) in diethyl ether than either iodo-Gilman ($R_2CuLi.LiI$) or salt-free (R_2CuLi) species [35,98]. The presence of such oligomeric units, possibly combined with the increased Li^+ Lewis acidity in the oligomeric form, has been correlated to the higher reactivity observed for cyanocuprates [18]. These oligomeric structures have been postulated to arise from the formation in solution of homodimeric $Cu_2Li_2R_4$ units linked by bridging LiCN groups [35,98]. An alternative model for higher aggregated cyano-Gilman reagents can be seen in the structure of the amidocuprate $[TMP_2CuLi.LiCN(THF)]_2$ (TMP = 2,2,6,6-tetramethyl-piperidine) in which two (R_2CuLi_2CN) units dimerize by means of donation of the lone pair on the cyano ligands to lithium centers on adjacent units, thus forming a central four-membered Li_2N_2 ring (Fig. 26) [99].

The cyanocuprate $[Ph_2Cu]_2[Cu_2(CN)_4Li_4(PPh_3)_4(THF)_{10}]$ has also been structurally characterized in the solid-state and contains a centrosymmetric $[Cu_2(CN)_4Li_4(PPh_3)_4(THF)_{10}]^{2+}$ cation and two ion-separate $[Ph_2Cu]^-$ anions (Fig. 27) [100]. The unusual

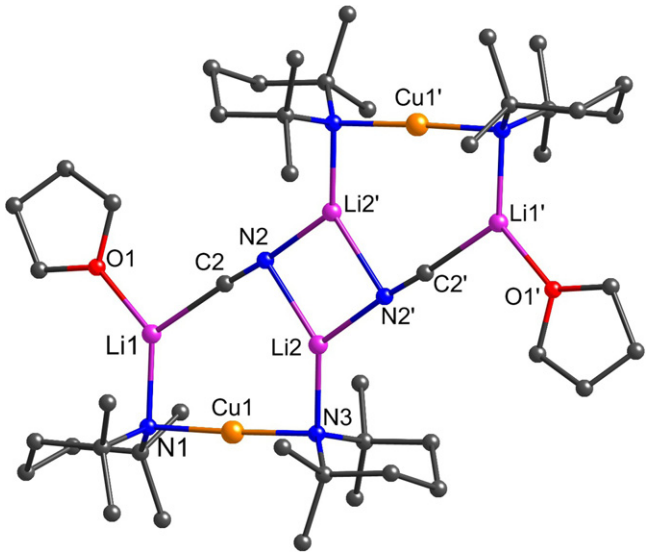

Fig. 26. Molecular structure of $[TMP_2CuLi.LiCN(THF)]_2$ [99].

cation can be envisaged as two $[Cu(CN)_2(PPh_3)_2]^-$ units aggregated together with four THF-solvated lithium cations, whereas the cuprate anions adopt a more orthodox linear arrangement (C_{ipso}–Cu–C_{ipso}, 174.8(4)°; mean Cu–C_{ipso} 1.915 Å). The complex was isolated from the 1:1:1 reaction mixture of phenyllithium, copper(I) cyanide and triphenylphosphane and is thus strictly speaking a lower-order cyanocuprate with a corresponding R(Ph):CN ratio of 1:1. However, instead of adopting heteroleptic RCuCNLi units reminiscent of other lower-order cyanocuprates (see Section 3.1), homoleptic $[R_2Cu]^-$ units, similar to those observed in cyano-Gilman reagents, are formed instead. This structural change can be attributed to the presence of the triphenylphosphane. Infra-red and low temperature NMR studies on the reaction mixture were also consistent with the formation of homoleptic $[Ph_2Cu]^-$ units in toluene/THF solution.

There are many reports in the literature of phosphanes being employed as additives in organocuprate chemistry in order to enhance the stability, selectivity and/or reactivity of organocuprates [9,10]. Reactivity studies on the above system demonstrate such an increase in reactivity, with the lower order cyanocuprate PhCuCNLi proving essentially inert in the 1,4-addition reaction to 2-cyclohexanone, however on addition of triphenylphosphane significantly increased reactivity was observed [100].

4. Lithium hetero-organocuprates

Heterocuprates are heteroleptic complexes possessing two different ligands in the cuprate unit, most usually an organo aryl or alkyl group and a hetero-atom based group. They were introduced as a means of combating one of main drawbacks associated with lithium homocuprate (Gilman) reagents, namely that in most applications one of the potentially valuable organo R groups remains attached to the copper center and is therefore not transferred to the substrate and is effectively wasted.

The stoichiometry of heterocuprates can be represented by the formula $LiCu(R_d)R_t$ where R_d is a non-transferrable or dummy group and R_t is an easily transferred organo group. In addition to cutting wastage of the organo group, many heterocuprates have been shown to have much improved thermal stabilities over homocuprates and are thus significantly easier to handle [10]. Moreover, the use of scalemic non-transferable groups has been much studied for applications in asymmetric synthesis [101].

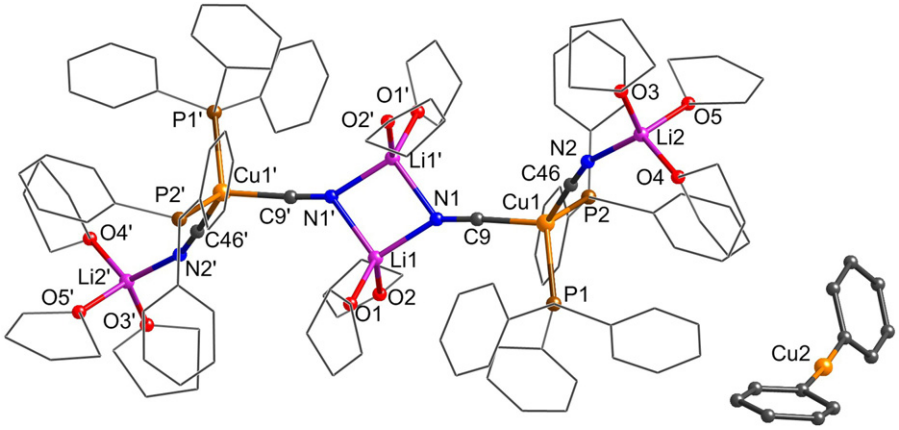

Fig. 27. Molecular structure of $[Ph_2Cu]_2[Cu_2(CN)_4Li_4(PPh_3)_4(THF)_{10}]$; only one of the two symmetry-related cuprate anions is shown for clarity [100].

The concept of heterocuprates was first introduced using alkynyl ligands as the non-transferable group (R_d = 1-alkynyl) [102]. However, these organo-alkynylcuprates were observed to be much less reactive than their corresponding homo-diorganocuprates. Subsequent studies led to the development of more reactive heterocuprates employing heteroatom based R_d groups [103], some of which have proven to be thermal stable even at ambient temperatures [104]. The reasons behind the non-transferability of the R_d groups was initially attributed to the strength of the Cu–R_d bond in these complexes, however computational studies have suggested that the reasons may be more subtle and rely both on the trans effect of the R_d ligand and on its ability to simultaneously bridge both copper and lithium centers in the transition state [105,106].

The most common synthetically utilized heterocuprates which also contain at least one organo group are detailed in Table 1. Silyl and stannyl cuprates differ somewhat from the other heterocuprates listed in that in these species it is the silyl or stannyl group which is transferred preferentially to the substrate rather than the organo group. Cyanocuprates can also be considered as a special class of heterocuprate, however for reasons already detailed these particular compounds have been considered separately in Section 3.

Despite their importance in synthesis, heterocuprates have been subject to far fewer studies than those reported for homocuprates. Indeed, at the time of writing there are no published solid-state structural characterizations available for $CuLi(R_d)R_t$ hetero-organocuprates with R_d = thio, alkoxy, aryloxy, thienyl, silyl or stannyl. The most studied of all heterocuprates are the amidocuprates, and these are therefore considered first.

4.1. Lithium organo-amidocuprates $LiCuR(NR'_2)$

Organo-amidocuprates differ from homocuprates ($LiCuR_2$) by replacement of one of the reactive organo groups (R) with a non-transferable amido group (NR'_2), thus giving heteroleptic $LiCuR(NR'_2)$ complexes. Organo-amidocuprates have been amongst the most synthetically utilized of all the heterocuprate species due to their high thermal stability and reactivity [9,10]. In addition, scalemic amidocuprates have attracted a lot of attention for applications in asymmetric conjugate addition reactions, although successes in this area to date have been somewhat limited [13,101,107]. These reagents have also found applications in the synthesis of substituted amines by means of oxidative coupling of the amido and organo groups [9,10,108]. Another recent synthetic application for which amidocuprates have shown promise is in the deprotonative cupration of functionalized benzenes, thus facilitating the preparation of regioselectively functionalized aromatics [99]. Several organo-amidocuprates have now been characterized in the solid state (Fig. 28) and also in solution.

Multinuclear NMR studies on organo-amidocuprates, and in particularly analysis of the multiplicity patterns and ^{15}N,^{6}Li NMR coupling constants in ^{15}N and ^{6}Li isotopically labeled samples, have strongly suggested the formation of dimeric structures in solution, similar to those observed for homocuprates (Section 2.1) [109–111]. Further evidence for the thermodynamic stability of the dimeric form was obtained in 2007 with the first reported solid-state characterization of an organo-amidocuprate $[Cu_2Li_2Mes_2(N(CH_2Ph)_2)_2]$ [112]. This complex was crystallized from the reaction mixture of copper mesityl and lithium dibenzylamide in toluene, and contains two $[RCuR_d]^-$ cuprate units lying anti-parallel, or head-to-tail, to one another (Fig. 29).

The $[Cu_2Li_2Mes_2(N(CH_2Ph)_2)_2]$ molecule sits on an inversion center, with both cuprates adopting a close-to-linear conformation (C–Cu–N, 175.3(2)Å). The Cu–C bond lengths (1.913(5)Å) are somewhat shorter than in the corresponding homocuprate $[Cu_2Li_2Mes_4]$ (av. 1.931(2)Å) [31], but are comparable to those

Table 1
Different classes of hetero-organocuprates.

Alkynylcuprates	$LiCuR(CCR')$
Thiocuprates	$LiCuR(SR')$
Alkoxy/Aryloxy-cuprates	$LiCuR(OR')$
Amidocuprates	$LiCuR(NR'_2)$
Phosphidocuprates	$LiCuR(PR'_2)$
Thienylcuprates	$LiCuR(C_4H_3S\text{-}2)$
Silylcuprates	$LiCuR(SiR'_3)$
Stannylcuprates	$LiCuR(SnR'_3)$

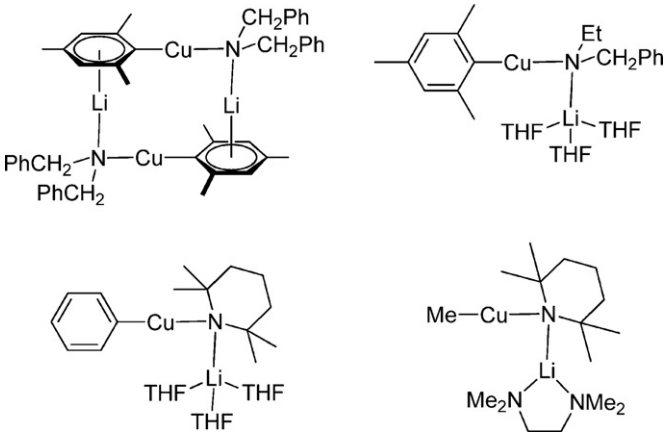

Fig. 28. Crystallographically characterized lithium organo-amidocuprates.

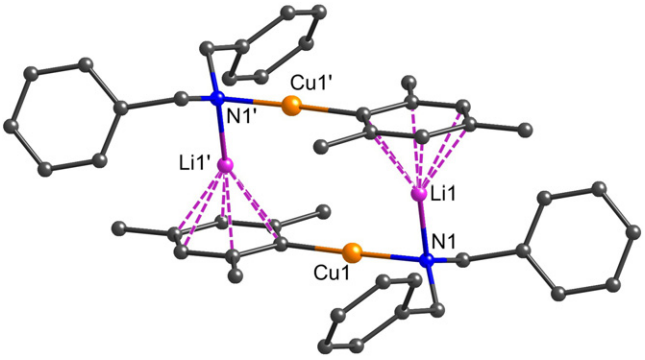

Fig. 29. Molecular structure of $[Cu_2Li_2Mes_2(N(CH_2Ph)_2)_2]$ [112].

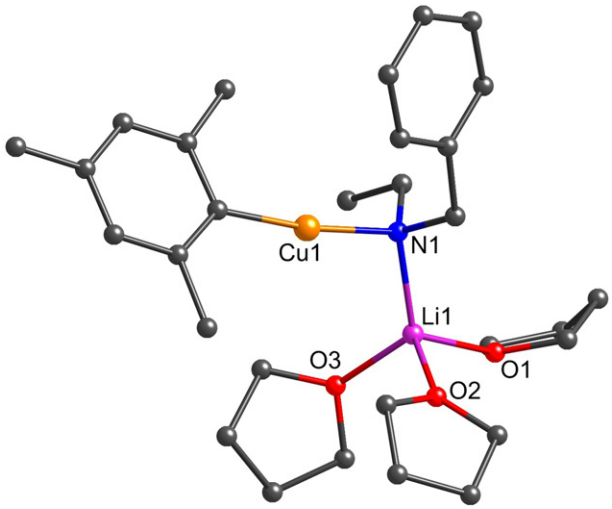

Fig. 30. Molecular structure of $[MesCu(N(Et)CH_2Ph)Li(THF)_3]$ [115].

reported for the $[CuMes_2]^-$ anion (1.915(9) Å) [43]. The Cu–N distance (1.921(4) Å) is significantly longer than Cu–N distances observed in homo-bis(amido)cuprates $[Cu(N(SiMePh_2)_2)_2]^-$ (mean 1.88 Å) [113], and $[Li(DME)Cu(NHMes)(NHPh)]_2$ (mean 1.855 Å; DME = dimethyoxyethane) [114], although the different amido groups make a direct comparison difficult. The lithium cations are coordinated to an amido nitrogen (Li–N, 1.969(10) Å) and are η^6 to a mesityl aryl ring (mean Li–C, 2.386 Å).

Solution state studies on $[Cu_2Li_2Mes_2(N(CH_2Ph)_2)_2]$ have provided key evidence of solution based equilibrium reactions for amidocuprates. Thus, ^{7}Li NMR spectroscopic studies on a toluene-d^8 solution of the 1:1 reaction mixture of CuMes and $LiN(CH_2Ph)_2$ revealed no less than five main lithium environments. With the aid of solution molecular mass measurements and inverse-detected ^{1}H–^{7}Li HOESY NMR spectroscopy these peaks were assigned to a number of different structural isomers: a head-to-tail isomer (similar to that observed in the solid state, Fig. 29), a head-to-head isomer, a mixed homocuprate isomer and the parent homo-diorganocuprate and homo-bis(amido)cuprate species (Scheme 8) [112]. These isomers were shown to exist together in solution in a Schlenk-type equilibrium, the most dominate species being the head-to-tail isomer. In agreement with these observations, computational studies have predicted the head-to-tail dimer to be the most thermodynamically favored isomeric form for simple organo-amidocuprates [112].

The presence of more than one isomer in solution is potentially significant for the synthetic applications of these reagents, especially since the most thermodynamically stable isomer is not necessarily the most kinetically reactive one. This is of particular relevance to asymmetric addition reactions involving chiral lithium amidocuprate reagents, and may in part explain the difficulties often encountered when trying to achieve high enantiomeric excesses with these reagents.

Lithium homocuprate structures have previously been shown to be highly dependent upon the solvent system (Scheme 3), and thus solvent effects have also been studied for the model amido-organocuprates $LiCu(R_t)R_d$ where R_t = Mes, $R_d = N(CH_2Ph)_2$ [115] and $R_t = n$Bu, R_d = N-methyl-1-phenyl-2-(1-pyrrolidinyl)ethanamine [111]. Unlike homocuprates whose contact ion pair (CIP) form undergoes dissociation in the presence of strongly lithium-coordinating solvents such as THF to give solvent separate ion pairs (SSIPs), addition of THF to organo-amidocuprates was shown, using 1D and 2D multinuclear NMR experiments, to lead to disaggregation of the dimer and the formation of solvated CIP monomers (Scheme 9) [111,115]. In addition, some decomposition to give the homo-metallic lithium amide and organocopper parent species was also observed for both complexes.

Three monomeric CIP organo-amidocuprate structures have been characterized in the solid state (Fig. 28). $[MesCu(N(Et)CH_2Ph)Li(THF)_3]$ was obtained from the reaction of copper mesityl with lithium *N*-benzylethylamide in toluene/THF (Fig. 30) [115]. The two-coordinate copper center is approximately linear (C–Cu–N, 171.98(16)°) and the Cu–C and Cu–N bond distances (1.907(4) and 1.912(3) Å respectively) are comparable to analogous bond distances in the corresponding amidocuprate dimer $[Cu_2Li_2Mes_2(N(CH_2Ph)_2)_2]$ (1.913(5) and

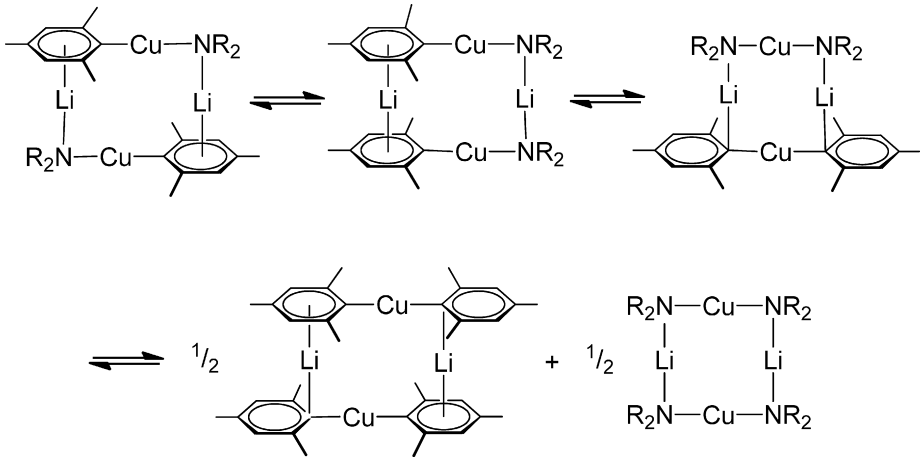

Scheme 8. Solution equilibrium for $[Cu_2Li_2Mes_2(NR_2)_2]$ R = CH_2Ph [112].

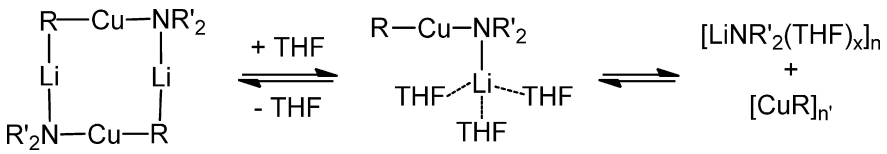

Scheme 9. Aggregation behavior of organo amidocuprates in THF [111,115].

1.921(4) Å; *vide supra*). The lithium center is tetrahedrally coordinated to the cuprate amido nitrogen (Li–N, 2.041(9) Å) and three THF oxygen atoms. The Li–N distance is therefore longer than that in both $[Cu_2Li_2Mes_2(N(CH_2Ph)_2)_2]$ (1.969(10) Å) and the parent lithium amide $[LiN(CH_2Ph)_2.THF]_2$ (1.983 Å) [116]. In addition, the angle described by Cu–N–Li is close to tetrahedral (106.5(3)°) and thus significantly more obtuse than the Cu–N–Li angle in $[Cu_2Li_2Mes_2(N(CH_2Ph)_2)_2]$ (90.0(3)°).

Retention of a CIP structure in THF, albeit in monomeric rather than dimeric form, has been attributed to a strong interaction between the nitrogen lone pair (which sits predominately in a $2p_z$ orbital) and the lithium cation, and this has been reasserted using theoretical calculations [115].

$[PhCuTMPLi(THF)_3]$ and [MeCuTMPLi(TMEDA)] (TMEDA = *N*,*N*,*N*′,*N*′-tetramethylethylendiamine) both exhibit similar structural features to those observed in $[MesCu(N(Et)CH_2Ph)Li(THF)_3]$ above [117]. However, it is interesting to note that both of these complexes were obtained from solutions which could effectively be considered as cyano-Gilman reaction mixtures. Thus $[PhCuTMPLi(THF)_3]$ was isolated from a 1:1:1 mixture of CuCN:PhLi:LiTMP in THF/toluene and [MeCuTMPLi(TMEDA)] was isolated from a similar 1:1:1 mixture of CuCN:MeLi:LiTMP in the presence of TMEDA and THF. In the case of cyano-Gilman cuprates formed from CuCN:2RLi, separated ion-pair structures of the form $[R_2Cu]^-[Li_2(CN)(THF)_x]^+$ are to be expected in THF (see Section 3.2). However here the stronger amido nitrogen–lithium interactions result in the isolation of monomeric CIP structures instead, and the cyano group is assumed to remain in solution as $[Li(CN)(THF)_x]$ [117].

4.2. Lithium organo-phosphidocuprates $LiCuR(PR'_2)$

Organo-phosphidocuprates of general stoichiometry $LiCuR(PR'_2)$ have, like organo-amidocuprates, been shown to be synthetically useful reagents with thermal stabilities significantly higher than those observed for the corresponding homo diorganocuprates or cyanocuprates [104]. Furthermore, organo-phosphido cuprates incorporating the bulky $P(tBu)_2$ group, whilst being only slightly less reactive than the corresponding diorganocuprates in conjugate addition to enones, can be stored in THF at ambient temperature for 4 h with less than 4% reported loss of activity, or even maintained at reflux for 4 h with less than 15% decomposition [118].

Only one crystallographically characterized organo-phosphidocuprate has been reported in the literature to date (Fig. 31): $[MeCuP(tBu)_2Li(THF)_3]$ [118] was prepared from the reaction $[CuP(tBu)_2]_4$ [119] with MeLi.LiBr. Although LiBr was not incorporated into the solid-state structure, its presence in the reaction mixture was required in order to obtain quantitative yields of the desired organo-phosphidocuprate.

Crystals of $[MeCuP(tBu)_2Li(THF)_3]$ show the complex to exist in the solid state in monomeric CIP units, similar to those observed for organo-amidocuprates in THF (Section 4.1). However, given the known preference for phosphido groups to form bridging bonds with copper centers [119,120], a monomeric structure is perhaps more surprising in this case. The coordination geometry of the copper center in the cuprate unit is approximately linear (C–Cu–P, 179.0(3)°). The Cu–C distance (1.940(4) Å) is close to that observed in $[CuMe_2]^-$ anions (av. 1.938 Å) [33,41,44], whilst the Cu–P bond length (2.217(2) Å) compares to a Cu–P distance of 2.209(5) Å in the phosphidocopper tetramer $[CuP(tBu)_2]_4$ and 2.266(4) Å in the homo-bis(phosphido)cuprate $[Cu(PtBu_2)_2Li(thf)_2]_\infty$ [118]. The lithium counter cation is associated with the distorted tetrahedral phosphorus center and three THF oxygen atoms. The Li–P distance (2.54(1) Å) is considerably shorter and stronger than that in $[Cu(PtBu_2)_2Li(thf)_2]_\infty$ (mean Li–P, 2.83 Å).

4.3. Lithium organo-alkynylcuprates $LiCuR(C{\equiv}CR')$

Although organo-alkynylcuprates were amongst the first heterocuprates to be reported, they tend to exhibit low reactivity in addition and substitution reactions and are only reactive at temperatures similar to those at which thermal decomposition occurs [102]. This has therefore limited their synthetic utility in these fields. Alkynylcuprates have, however, proven more promising for oxidative cross-coupling synthetic protocols, for example in the preparation of polyfunctional alkynes [121,122]. Several lithium organo-alkynylcuprates have been characterized in the solid-state, two of which exhibit dimeric structures and one a monomeric structure (Fig. 32).

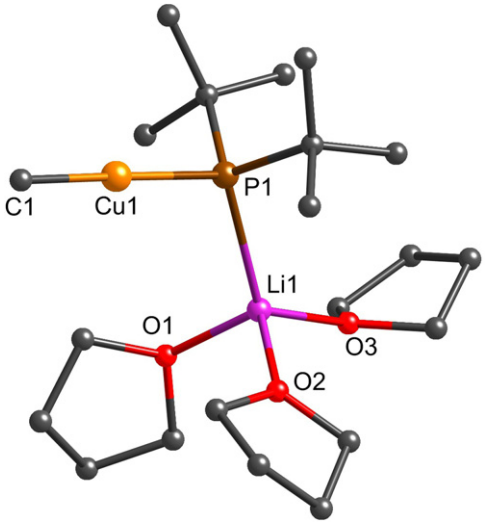

Fig. 31. Molecular structure of $[MeCuP(tBu)_2Li(THF)_3]$ [118].

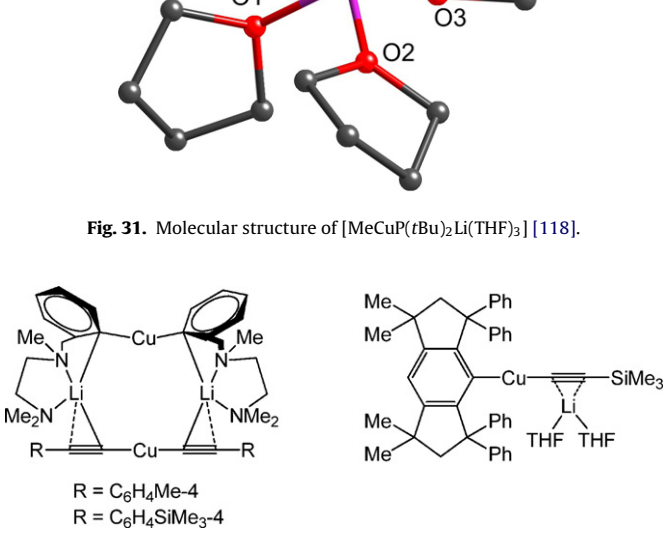

Fig. 32. Crystallographically characterised lithium organo-alkynylcuprates.

The alkynylcuprates $[Cu_2Li_2(Ar)_2(C{\equiv}CC_6H_4Me)_2]$ and $[Cu_2Li_2(Ar)_2(C{\equiv}CC_6H_4SiMe_3)_2]$ (Ar = $C_6H_4(CH_2N(Me)CH_2CH_2NMe_2)$-2) were prepared from the equimolar reaction of LiAr with copper(I) *p*-tolylacetylide or copper(I) *p*-trimethylsilylacetylide in toluene respectively [123]. Both complexes have identical structural geometries, comprising of two different homocuprate units, a dialkynyl cuprate and a diaryl cuprate, joined together by two lithium cations.

In the solid-state structure of $[Cu_2Li_2(Ar)_2(C{\equiv}CC_6H_4Me)_2]$ (Fig. 33) each of the cuprate units are orientated mutually orthogonal to one another, and show close to linear geometry at the copper centers (Ar–Cu–Ar, 173.15(9)°; RCC–Cu–CCR, 166.91(9)°). The (aryl)C_{ipso}–Cu bonds, mean 1.933 Å, are significantly longer than the (acetylide)C_α–Cu bonds, mean 1.869 Å, reflecting the differences in hybridization between the two carbon atoms (sp^2 and sp respectively). The two lithium atoms are tetrahedral four-coordinated by the *ipso*-carbon atom of an aryl anion (mean C_{ipso}–Li, 2.506(4) Å), the α-carbon of an acetylide anion (mean C_α–Li, 2.226 Å), and by a *N*,*N*′-chelated diamine functionality of the *ortho*-$C_6H_4CH_2N(Me)CH_2CH_2NMe_2$ substituent (mean Li–N, 2.073 Å). The (aryl)C_{ipso}–Li distances are therefore significantly longer than the (alkynyl)C_α–Cu distances and are also longer than the (aryl)C_{ipso}–Li bonds in the related diaryl cuprate complex $[Cu_2Li_2(C_6H_4CH_2NMe_2\text{-}2)_4]$, 2.385(7) Å [25]. A side-on bridging interaction between the acetylide unit and the lithium center was also proposed based on a relatively short Li–C_β distance of 2.7 Å in the solid-state structure, and also upon the observation of ^{13}C–^{7}Li coupling in the ^{13}C NMR solution spectrum. As a result of their coordination to the lithium atoms, two of the amino nitrogens in $[Cu_2Li_2(Ar)_2(C{\equiv}CC_6H_4Me)_2]$ are stereogenic and the solid-state structure contains an S_NS_N/R_NR_N enantiomeric pair.

Cryogenic molecular mass measurements in combination with NMR and Infra-red spectroscopic studies all indicated that the mixed homo-cuprate motif observed in the solid-state structures of $[Cu_2Li_2(Ar)_2(C{\equiv}CC_6H_4Me)_2]$ and $[Cu_2Li_2(Ar)_2(C{\equiv}CC_6H_4SiMe_3)_2]$ are maintained in solution [123]. Unlike the previously discussed organo-amidocuprate $[Cu_2Li_2Mes_2(N(CH_2Ph)_2)_2]$ (see Section 4.1) no other structural isomers were observed, and no Schlenk-type equilibrium was perceived. Moreover, the mixed homocuprate structure was shown to be by far the most thermodynamically stable product, being the only mixed-metal product formed irrespective of the ratio of copper to lithium starting material used. How much of this behavior can be attributed to the presence of the *N*,*N*′-chelating diamine functionalities is unclear.

In contrast to the dimeric mixed homo-cuprate structures discussed above, $[(MPhind)CuC{\equiv}CSiMe_3.Li(THF)_2]$ (in which the aryl MPhind ligand is based on rigid fused-ring *s*-hydrindacenyl

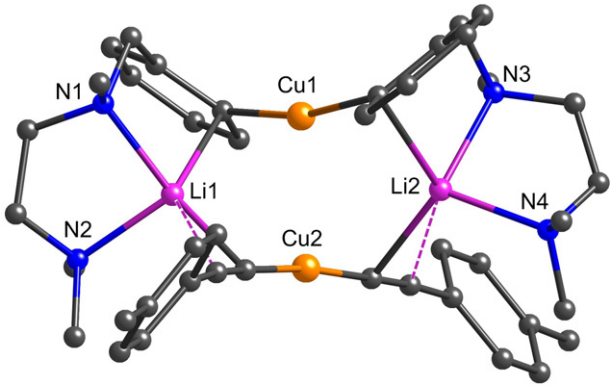

Fig. 33. Molecular structure of $[Cu_2Li_2(Ar)_2(C{\equiv}CC_6H_4Me)_2]$; Ar = $C_6H_4(CH_2N(Me)CH_2CH_2NMe_2)$-2 [123].

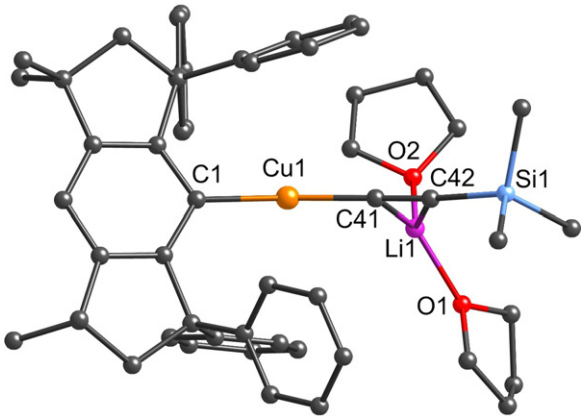

Fig. 34. Molecular structure of $[(MPhind)CuC{\equiv}CSiMe_3.Li(THF)_2]$ [122].

skeleton) adopts a monomeric solid-state structure with a heteroleptic cuprate moiety (Fig. 34) [122]. The copper center in the heterocuprate unit is bound to one aryl ligand and one alkynyl ligand in a close to linear geometry (C–Cu–C, 165.40(11)°). The Cu–C(sp^2) and Cu–C(sp) distances of 1.942(2) and 1.871(3) Å respectively, are close in magnitude to the corresponding bond distances reported for the mixed homo-cuprate complexes discussed above. The lithium is associated to the cuprate unit to form a contact ion pair by means of η^2 coordination to the two carbon atoms of the acetylene unit (Li–C, 2.135(6) and 2.385(7) Å), and is also additionally coordinated by the oxygen atoms of two THF solvate molecules.

4.4. Lithium organo-halocuprates LiCuR(X)

Treatment of a copper(I) halide with an equimolar amount of organolithium reagent typically leads to the formation of a new organocopper compound and elimination of the lithium halide salt (Scheme 2). However, the use of sterically bulky organo groups in order to disfavor $(CuR)_n$ organocopper aggregate formation, has been shown in some cases to facilitate the isolation of the heteroleptic organo-halocuprate species instead. Two lithium organo-iodocuprates and two lithium organo-bromocuprates have been isolated and characterized in the solid state (Fig. 35).

The organo-iodocuprate $[(C_6H_3Trip_2\text{-}2,6)CuILi(OEt_2)_2]$ (Trip = $C_6H_2iPr_3$-2,4,6) was isolated from the reaction mixture of copper(I) iodide with one equivalent of $Li(C_6H_3Trip_2\text{-}2,6)$ in diethyl ether [124]. The cuprate adopts a monomeric contact ion pair motif with a two-coordinate copper (C–Cu–I, 171.4(2)°) and Cu–I and Cu–C distances of 2.4512(8) and 1.902(5) Å respectively (Fig. 36). The Cu–C bond is therefore similar in length to that reported in the closely related lower-order cyanocuprate $[(C_6H_3Trip_2\text{-}2,6)CuCNLi(THF)_2]_2$ (1.906(4) Å; see Section 3.1) [78]. The lithium cation is tri-coordinate to an iodide anion (Li–I, 2.69 Å) and two solvate Et_2O molecules, with an unexpectedly compressed Cu–I–Li angle of 95.5(2)°.

A similar contact ion pair motif has been reported for the organo-bromocuprate complex $[MPhindCuBrLi(THF)_3]$ [122]. The copper is once more is close to linear in geometry (C–Cu–Br, 177.34(11)°), whilst the bonding at the halide center is now much more obtuse (Cu–Br–Li, 110.64(19)°). Other relevant bond lengths are: Cu–C, 1.916(4) Å; Cu–Br, 2.2569(7) Å; and Br–Li, 2.444(9) Å.

Two separated ion pair organo-halocuprates have also been structurally characterized in the solid state. $[(Me_3Si)_2CHCuBr][Li(12\text{-crown-}4)_2]$ was isolated from solution after addition of 12-crown-4 to a mixture of $LiCH(SiMe_3)_2$ and copper(I) bromide [41]. The C–Cu–Br angle is near linear, 178.7(2)°, and the Cu–C distance of 1.920(6) Å is slightly shorter than compa-

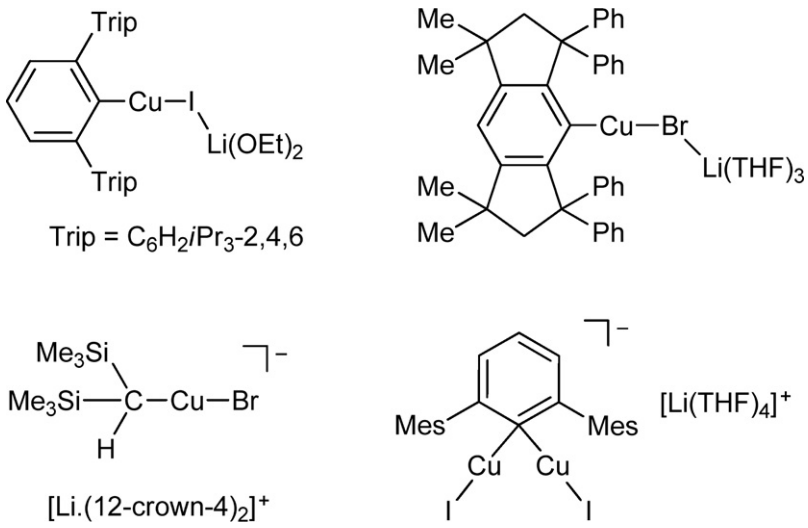

Fig. 35. Crystallographically characterized lithium halo-organocuprates.

rable Cu–C distances in the homocuprate anion ($[Cu(CH_2SiMe_3)_2]^-$ (1.937 Å)) [33]. The Cu–Br distance is 2.267(2) Å.

The other separated ion pair species, $[Cu_2I_2(C_6H_3Mes_2$-2,6)$]^-[Li(THF)_4]^+$, was prepared from the treatment of copper(I) iodide with two equivalents of $Li(C_6H_3Mes_2$-2,6) in diethyl ether/THF [124]. The anion in this complex (Fig. 37) is therefore very different in stoichiometry and structure to that observed in other hetero-organocuprates, comprising of two copper iodide units slightly asymmetrically bridged by the *ipso*-carbon of an aryl group (av. C–Cu = 1.971(15); Cu–I, 2.419 Å). The copper centers are somewhat distorted from linear with I–Cu–C angles of 164.1(4) and 166.8(1)°. The bending of the geometry at the copper centers highlights the short Cu···Cu separation of 2.391(3) Å, however this cannot be used to imply the presence of Cu–Cu bonding and instead is better ascribed to iodine–iodine repulsions [124].

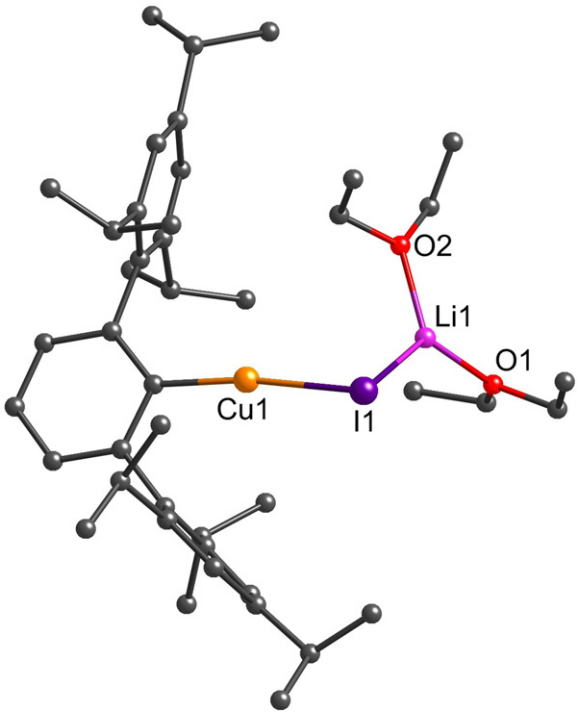

Fig. 36. Molecular structure of $[(C_6H_3Trip_2$-2,6)CuILi$(OEt_2)_2]$ [124].

5. Magnesium organocuprates

Much of the early research on the preparation and properties of organocuprate complexes involved the use of magnesium Grignard reagents (RMgX, X = halide) as the source of the organo group, thus giving organocuprates with the general stoichiometry R_2CuMgX [3]. Research on magnesium–copper reagents has continued apace and their synthetic utility has often been shown to rival or even exceed that of their lithium analogues in many applications [9,10]. For example, the use of Grignard reagents in copper(I) catalyzed asymmetric addition reactions is now a well-established synthetic protocol [125–127].

However, in stark contrast to recent advances in the understanding of lithium organocuprates (see Sections 2, 3 and 4), the structures of the equally ubiquitous Grignard-derived magnesium organocuprates have remained relatively unreported. Nevertheless, in recent years several attempts have been made to address this, and a number of magnesium organocuprate structures have now been structurally characterized in the solid state (Fig. 38).

Initial solution studies on the reaction mixture of copper(I) bromide with bis(aryl)magnesium species in THF or diethyl ether predicted the formation of discrete metal clusters of the form Cu_4MgAr_6 (where Ar was either a phenyl or *para*-tolyl group) [128]. This was later verified by the isolation and solid-state characterization of the magnesium cuprate complex $[Ph_6Cu_4Mg(OEt_2)]$ (Fig. 39) [63]. The cluster is based upon a trigonal bipyramidal arrangement

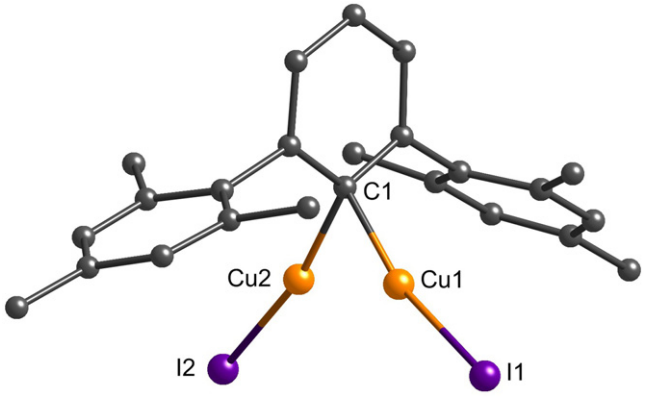

Fig. 37. Molecular structure of the cuprate anion in $[Cu_2I_2(C_6H_3Mes_2$-2,6)$][Li(THF)_4]$ [124].

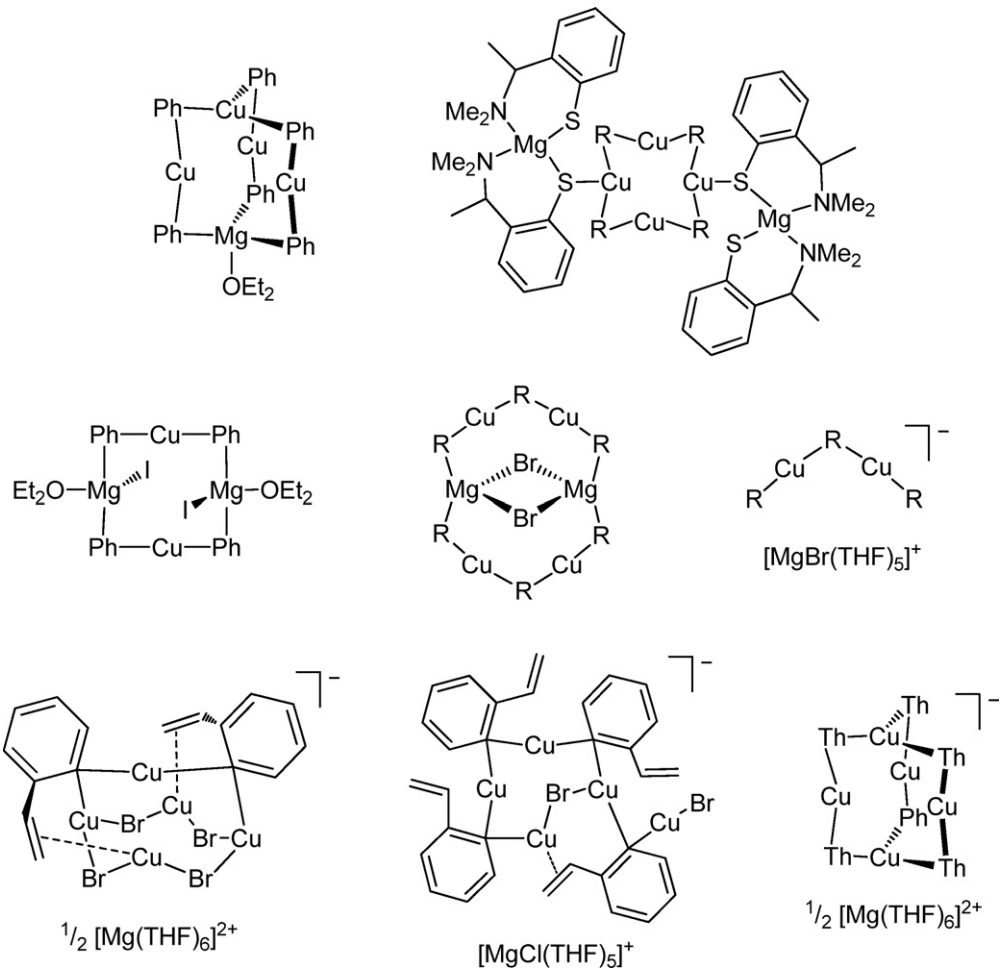

Fig. 38. Crystallographically characterized magnesium organocuprates (R = C_6H_2Me-2,4,6; Th = C_4H_3S-2).

of metal atoms with three copper atoms in equatorial positions and copper and magnesium atoms in the apical positions. The six phenyl groups each bridge two metal centers *via* their C_{ipso} carbon atoms (mean distances: Mg–C, 2.35(1); Cu_{ax}–C, 2.09(1); Cu_{eq}–C, 1.95(1) Å). The structure is best considered as three close to linear (160.9(4)° at Cu) Ph_2Cu^- cuprate units each centered on an equatorial copper center. These are joined together at the apical positions by the Cu^+ and Mg^{2+} cations. This structure is therefore directly analogous to the lithium organocuprate $[Cu_4LiPh_6]^-$ (see Fig. 15b) [63] although the larger size of the magnesium compared to lithium results in the magnesium being displaced out of the plane of the three coordinating C_{ipso} atoms by approximately 0.4 Å. The magnesium is additionally coordinated by a solvate diethyl ether molecule, thus giving rise to a distorted tetrahedral coordination geometry.

A very different structural motif was reported for $[Cu_4Mes_4(SC_6H_4(CHMeNMe_2)\text{-}2)_4Mg_2]$ (Fig. 40), which was formed from the treatment of the thiophenolato copper species $[CuSC_6H_4(CHMeNMe_2)\text{-}2]$ with the diarylmagnesium reagent $[Mg(Mes)_2(THF)_2]$ [129,130]. The solid-state structure is based upon a central Cu_4Mes_4 tetrameric moiety, similar to that observed in the solid-state structure of $[Cu_4Mes_4]$ [66]. Peripherally to this core are two bis(thiophenolato)magnesium units. The magnesium atoms within these units are approximately tetrahedral coordinated, being S,N chelated by each of the two thiophenolato ligands. In addition, the sulfur atom in one of the thiophenolate ligands bridges to one of the copper centers in the Cu_4Mes_4 moiety. Although one possible interpretation of this structure would involve the presence of $[CuR_2R_d]^{2-}$ higher-order cuprate centers – where R is the mesityl group and R_d is the heteroatom based ligand $SC_6H_4CHMeNMe_2$ – such a scenario seems unlikely. Instead the structure is best considered as being analogous to the organocopper tetramers $[Cu_4Ph_4(SMe_2)_2]$ [28] and $[Cu_4Mes_4(THT)_2]$ (THT = tetrahydrothiophene) [131] in which the SMe_2 or THT ligand is replaced by one of the sulfur atoms from a neutral $Mg(SC_6H_4CHMeNMe_2)_2$ unit. Moreover, the observed Cu–S distance of 2.389(2) Å is directly comparable to Cu–S distances of 2.383 (2) Å in $[Cu_4Ph_4(SMe_2)_2]$ and 2.409 Å (mean) in $[Cu_4Mes_4(THT)_2]$. NMR studies indicate that $[Cu_4Mes_4(SC_6H_4(CHMeNMe_2)\text{-}2)_4Mg_2]$ breaks up in solution into its homometallic components, with interaggregate exchange of aryl and thiophenolato ligands evident at higher temperatures [130].

Both of the magnesium organocuprates discussed above was prepared using diorganomagnesium reagents as the source of the organo group. However, magnesium organocuprates used in synthetic protocols are predominately derived from the far more readily available Grignard reagents. It is therefore unclear how well the above structures can correlate to the species present in actual Grignard derived organocuprate reaction mixtures.

The first structural determination of a Grignard-derived contact ion pair organocuprate was recently reported in 2008 [132]. Reaction of mesityl copper with phenyl magnesium iodide in diethyl ether gave a solution from which crystals of $[Ph_4Cu_2(Mg(OEt_2)I)_2]$ were obtained. X-ray crystallography revealed a centrosymmetric dimer, consisting of two $[Ph_2Cu]^-$ cuprate anions connected

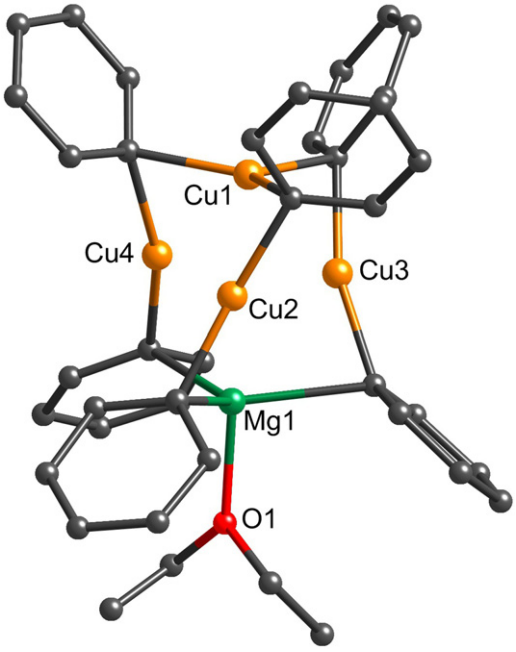

Fig. 39. Molecular structure of $[Ph_6Cu_4Mg(OEt_2)]$ [63].

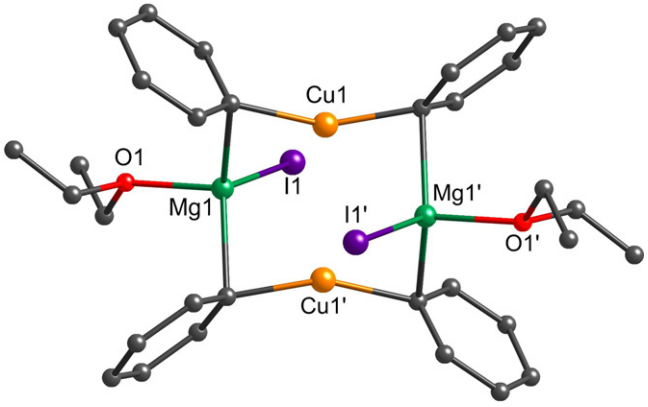

Fig. 41. Molecular structure of $[Ph_4Cu_2(Mg(OEt_2)I)_2]$ [132].

together *via* Et_2O-solvated $[MgI]^+$ monocations (Fig. 41). The magnesium metal centers are approximately tetrahedral with the magnesium-coordinated iodides lying one above and one below the central eight membered $Cu_2Mg_2C_4$ ring (Mg–I, 2.7046(10) Å). The structure is therefore isostructural to the previously reported lithium diphenylcuprate $[Ph_4Cu_2Li_2(OEt_2)_2]_2$ [27] (see Fig. 3a) with the lithium cations formally replaced by $[MgI]^+$ mono-cations, thus demonstrating that magnesium Grignard diorganocuprates are able to form analogous CIP structures to lithium diorganocuprates.

The Cu–C distances in $[Ph_4Cu_2(Mg(OEt_2)I)_2]$ (mean 1.942(3) Å) are comparable to those in $[Ph_4Cu_2Li_2(OEt_2)_2]_2$ and other lithium diarylcuprates (range 1.906(5) to 1.948(3) Å; see Section 2.1). However, at 156.97(13)° the C–Cu–C bond angle is noticeably less obtuse than in these lithium diarylcuprates. This can be attributed to the higher degree of covalency in the Mg–C_{ipso} bond leading to a corresponding increase in Cu–C_{ipso}–Mg 3 center–2 electron bonding character. The mean Mg–C distance is 2.276 Å and therefore significantly shorter than Mg–C distances in $[Cu_4MgPh_6(OEt_2)]$ (mean Mg–C 2.35(1) Å) [63], in which the magnesium center bridges three phenyl groups.

A contact ion pair arrangement was also reported in the solid-state structure of $[Cu_4Mg_2Mes_6Br_2]$ which was isolated from the reaction mixture of mesityl copper with mesityl magnesium bromide in diethyl ether/toluene [132]. The crystals contained two structurally identically but independent complexes in the asymmetric unit (one of which is shown in Fig. 42). The cuprate is formally an aggregation of two $[MgBr]^+$ cations and two $[Cu_2Mes_3]^-$ anions, and can thus be considered as a dimer similar to $[Ph_4Cu_2(Mg(OEt_2)I)_2]$ but with the $[Ph_2Cu]^-$ units replaced by $[Mes_3Cu_2]^-$ units. The difference in the makeup of these cuprate anions can be explained by the increased steric requirement of the mesityl group over the phenyl group, thus inhibiting the formation of any possible dimeric $[Mes_4Cu_2(MgBr)_2]$ structure due to the steric clash between *ortho*-CH_3 groups on the mesityl ring and bromide atoms. It is also possible to consider the structure as a novel type of "inverse crown ether" in which a 12-membered $[Cu_4Mg_2C_6]^{2+}$ macrocycle encapsulates two bromide guest anions [132,133].

The magnesium centers in $[Mes_6Cu_4Li_2Br_2]$ are approximately tetrahedral and form a central four-membered Mg_2Br_2 ring with the two bromide atoms (mean Mg–Br, 2.5707 Å). Mg–C distances (mean, 2.268 Å) are comparable in length to those in $[Ph_4Cu_2(Mg(OEt_2)I)_2]$. Two different types of mesityl groups are present: the first type bridges two copper atoms symmetrically to give a 3 center–2 electron Cu–C–Cu bond (mean Cu–C, 1.994 Å), whereas the second type asymmetrically bridges both a Mg and Cu center, thus forming shorter Cu–C contacts (mean 1.964 Å). The mean angle at the two-coordinate copper centers is 156.63°.

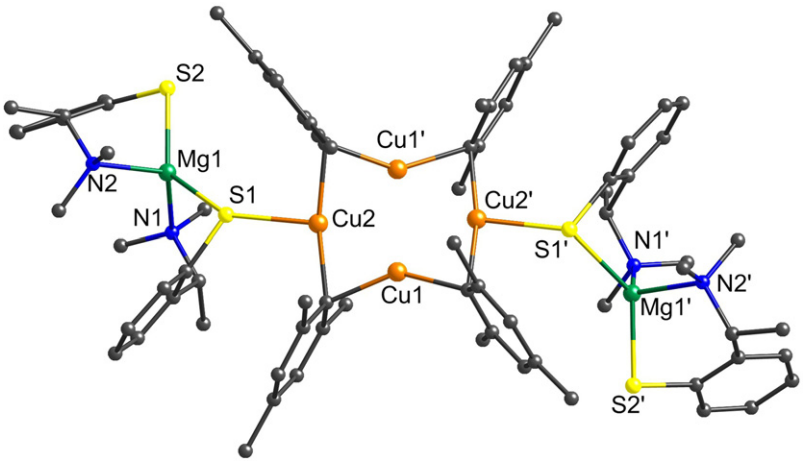

Fig. 40. Molecular structure of $[Cu_4Mes_4(SC_6H_4(CHMeNMe_2)\text{-}2)_4Mg_2]$ [129,130].

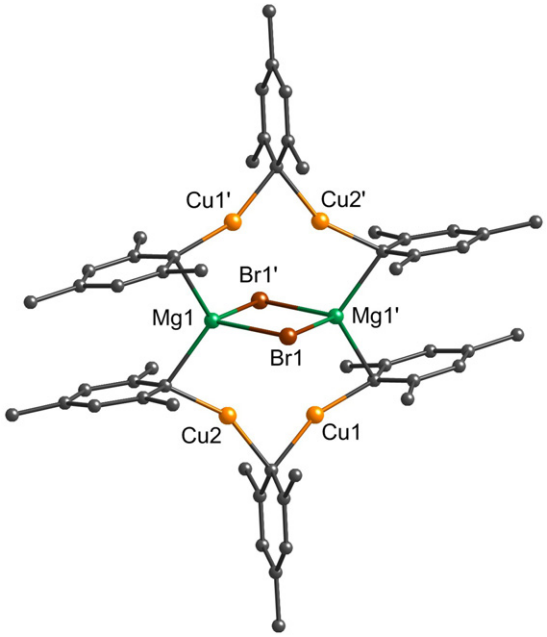

Fig. 42. Molecular structure of $[Cu_4Mg_2Mes_6Br_2]$ [132].

Repetition of the same reaction between mesityl copper and mesityl magnesium bromide but using THF in place of diethyl ether gave crystals of $[Cu_2Mes_3]^-$ $[MgBr(THF)_5]^+$ [132]. This separated ion pair structure comprises of a cation containing an octahedral magnesium center coordinated to five THF molecules and one bromide, and a dimetallic $[Cu_2Mes_3]^-$ anion (Fig. 43). The anion is unique, containing two terminal mesityl groups which can be considered to form short 2 center–2 electron bonds with the copper atoms (mean length, 1.924(8) Å), and one mesityl group which bridges both copper centers by way of an approximately symmetric 3 center–2 electron Cu–C–Cu bond, thus giving longer copper–carbon distances (mean 2.012 Å). Although there are no other examples of $[Cu_2R_3]^-$ anions in organocopper chemistry, the silylcuprate $[((Me_3Si)_3Si)_3Cu_2]$ [134] forms an analogous structure, and the organo-iodocuprate $[Cu_2I_2(C_6H_3Mes_2\text{-}2,6)][Li(THF)_4]$ [124] (see Section 4.4) adopts a similar arrangement but with iodide

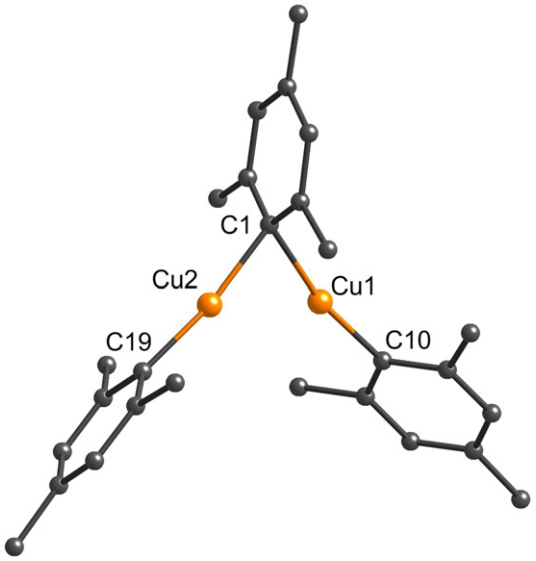

Fig. 43. Molecular structure of the anion in $[Cu_2Mes_3][MgBr(THF)_5]$ [132].

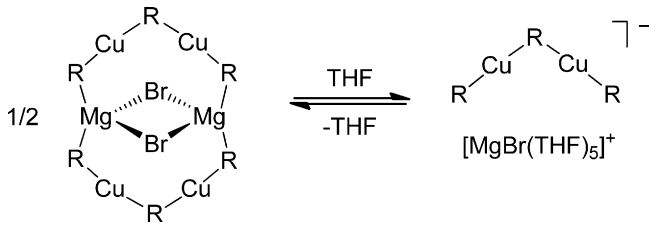

Scheme 10. Predicted CIP–SSIP equilibrium for $[R_6Cu_4Li_2Br_2]$ (R = $C_6H_2Me_3$-2,4,6) [132].

atoms instead of organo groups in the terminal positions. The angles at the copper centers in $[Cu_2Mes_3]^-$ are 168.0(3) and 171.0(3)°, and the Cu–C–Cu angle at the bridging *ipso*-carbon is 75.1(3)°. This gives rise to a short intramolecular Cu···Cu distance of 2.4515(14) Å.

The structures of $[Mes_6Cu_4Li_2Br_2]$ and $[Mes_3Cu_2][MgBr(THF)_5]$ can be considered together as CIP and SSIP structures of the same compound (Scheme 10) [132]. This again hints at close parallels between the behavior of lithium and Grignard-derived magnesium organocuprates, whereby CIP structures are favored in weakly coordinating solvents such as diethyl ether, whereas SSIP structures are favored in more strongly donor solvents such as THF (see Section 2.2).

Two Grignard-derived organocuprates incorporating *ortho*-vinylphenyl (viph) aryl groups have also been reported which have Cu:Mg ratios of 5:1 and 10:1 [135]. Accordingly reaction of copper(I) chloride with (viph)MgBr in THF led to the isolation of two mixed halide/aryl structures: $[Cu_5Br_2(C_6H_4CHCH_2\text{-}2)_4][MgCl(THF)_5]$ and $[Cu_5Br_4(C_6H_4CHCH_2\text{-}2)_2]_2[Mg(THF)_6]$ [135]. Both structures are ion separate species containing octahedrally coordinated magnesium-based cations and homometallic cuprate anions. The five metal centers within the $[Cu_5Br_2(viph)_4]^-$ and $[Cu_5Br_4(viph)_2]^-$ cuprate clusters adopt a square based pyramid geometry, the base of which is contains four copper centers in either a $Cu_4(viph)_3Br$ or Cu_4Br_4 eight-membered ring, with the apex occupied by a copper center in a (viph)CuBr or $(viph)_2Cu$ cuprate moiety respectively (Fig. 44). Within $[Cu_5Br_4(viph)_2]^-$ both of the vinylic groups are involved in intramolecular π-coordination of copper centers, whereas in $[Cu_5Br_2(viph)_4]^-$ only one of the four vinylic groups participates in π-coordination. These clusters can also be considered as structurally distorted analogues of $[Cu_5Ph_6]^-$ (see Section 2.4) [62] in which some of the aryl groups have been replaced with bromides.

A magnesium organocuprate with a 10:1 Cu:Mg ratio has also been obtained from the reaction of bromo-magnesium thienyl (BrMgTh; Th = C_4H_3S) with copper(I) chloride [136]. This reaction yielded $[Cu_5Th_6]_2[Mg(THF)_6]$; a separated ion pair complex comprising of a magnesium cation octahedrally coordinated by six THF molecules and a pentametallic trigonal bipyramidal $[Cu_5Th_6]^-$ cuprate anion, structurally analogous to $[Cu_5Ph_6]^-$ (see Section 2.4) [62].

6. Organocuprates with other metal centers

Although simple organocopper reagents are commonly prepared from the corresponding lithium or Grignard organometallics, the high basicity and nucleophilicity of both of these reagents make them incompatible with many functional groups. The use of either of these reagents therefore precludes the preparation of many functionalized organocopper compounds. One solution to this problem is the adoption of alternative organometallic precursors, and in principle any metal less electronegative than copper can be used. Some of the most studied species in this context include organo-zinc, -aluminum, -tin, -titanium and -zirconium compounds [10,13,14]. The desired organocopper reagent can be

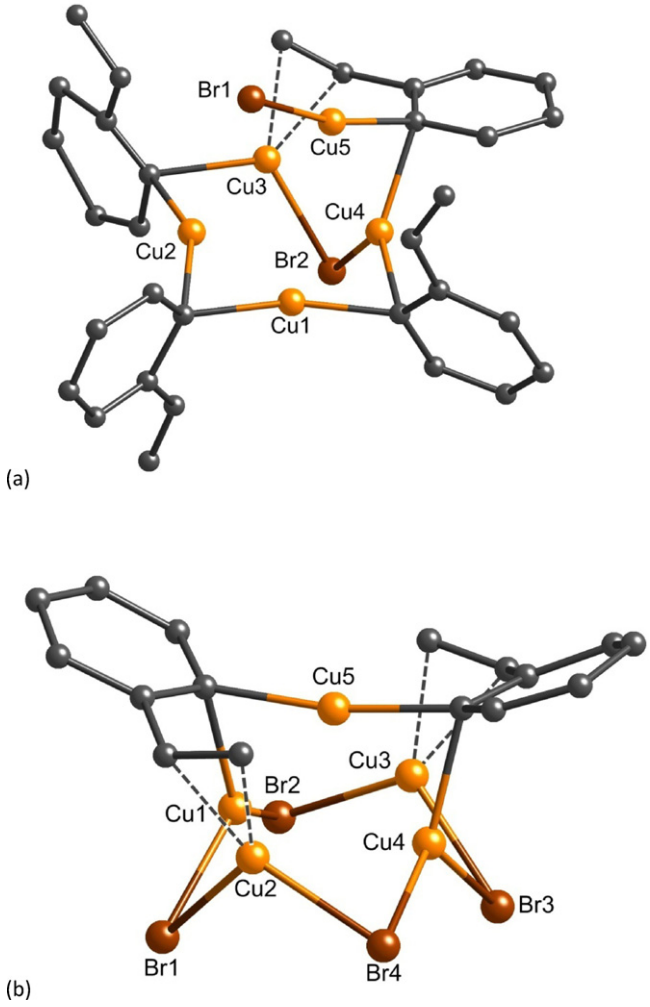

Fig. 44. Molecular structure of the cuprate anions in (a) $[Cu_5Br_2(C_6H_4CHCH_2\text{-}2)_4][MgCl(THF)_5]$ and (b) $[Cu_5Br_4(C_6H_4CHCH_2\text{-}2)_2]_2[Mg(THF)_6]$ [135].

prepared by reaction of an equimolar amount of one of these organometallics with a copper(I) salt, or alternatively in some cases the organometallic can also be used in catalytic copper systems in direct combination with an electrophile [127,137].

Notwithstanding the significant number of synthetic studies utilizing these alternative heterometallic organocopper based systems, there are in point of fact very few structurally characterized examples of heterometallic organocuprates which do not involve either lithium or magnesium. Nevertheless, the solid-state structures of a potassium lower order cyanocuprate and a calcium arylcuprate have both been conveyed. In addition, two heterotrimetallic cuprates involving lithium cations and ferrocenylene dianions have also been structurally characterized.

The lower-order lithium cyanocuprate RCuCNLi, where $R = (Me_2PhSi)_3C$, has been shown to adopt either a monomeric $[RCuCNLi(THF)_3]$ or dimeric $[RCuCNLi(THF)_2]_2$ motif in the solid state, both of which contain linear C–Cu–CN cuprate units (see Section 3.1) [80]. The heavier sodium and potassium analogues of this cyanocuprate have also been prepared *via* treatment of a THF suspension of copper(I) cyanide with $NaC(SiMe_2Ph)_3$ or $KC(SiMe_2Ph)_3$ respectively [80]. NMR and Infra-red studies indicated the sodium derivative to form a similar dimeric structure to the lithium complex. However in contrast, crystallographic characterization revealed the potassium derivative to adopt a tetrameric form (Fig. 45). Four approximately linear cyanocuprate units (mean C–Cu–C, 175.9°) assemble end-on into a tetramer by means of coordination of the potassium cations from the nitrogen end of their cyanide ligands. This gives rise to the formation of a central distorted K_4N_4 cube in which each potassium bridges three cyanide nitrogens and is further coordinated by η^6 and η^2 interactions with the π-system on an adjacent $C(SiMe_2Ph)_3$ ligand. Although the influence of the Group 1 metal on reactivity and selectivity for this particular series of lower-order cyanocuprates remains unreported, it should be noted that aggregation state has been shown to be one factor that can potentially play a large role in the reactivity of organocuprate reagents [18].

Moving on to Group 2 organocopper derivatives, a calcium organocuprate, $[Ph_3Ca_2(THF)_6]^+[Ph_2Cu]^-$, has been crystallized from the reaction mixture of calcium metal with phenyl copper [138]. The calcium was activated prior to reaction *via* dissolution in liquid ammonium followed by drying under vacuum in the absence of ammonia. The structure forms a solvent-separated ion pair containing a diphenylcuprate anion structurally analogous to cuprate anions observed in lithium solvent-separated diarylcuprates (see Section 2.2). The cuprate unit is strictly linear due to crystallographic inversion symmetry and the Cu–C distances are 1.910(3) Å. The identity of the cationic species is more unusual, containing aryl groups in addition to the calcium center and solvent molecules. Each calcium in $[Ph_3Ca_2(THF)_6]^+$ is hexa-coordinate to three terminal THF molecules and three bridging phenyl groups (mean Ca–C, 2.614 Å) which thus form 3 center–2 electron Ca–C–Ca bonds.

Two trimetallic lithium ferrocenylenecuprates have also been reported from the treatment of ferrocene with butyllithium and mesityl copper. Depending upon the choice of base, *t*BuLi or *n*BuLi/TMEDA, crystals of either $[(1,1'\text{-Fc})_2Cu_2Li_2(THF)_6]$ or $[(1,1'\text{-Fc})_6Cu_4Li_6][Li(THF)_4]_2$ (Fc = ferrocenylene) were obtained [139]. Although trimetallic in nature, both complexes are strictly speaking lithium homocuprates in which the organo R groups have been substituted by a dianionic organometallic 1,1′-ferrocenylene fragment. In addition, both lithium ferrocenylencuprates demonstrated interesting reactivity and were shown to undergo oxidative coupling to give poly-1,1′-ferrocenylene [139].

The molecular structure of $[(1,1'\text{-Fc})_2Cu_2Li_2(THF)_6]$ conforms to the accustomed R_2CuLi formulation for lithium organocuprates, the only difference being that one formula unit of dianion (the ferrocenylene unit) is present instead of two mono-anionic R groups (Fig. 46). Within the structure the C–Cu–C angle is almost linear (176.56(12)°), and the mean Cu–C bond distance (1.915 Å) is comparable to that in diaryl cuprates such as $[CuPh_2]^-$ (range 1.900(11)–1.931(11) Å; see Section 2.2). The cyclopentadienyl (Cp)

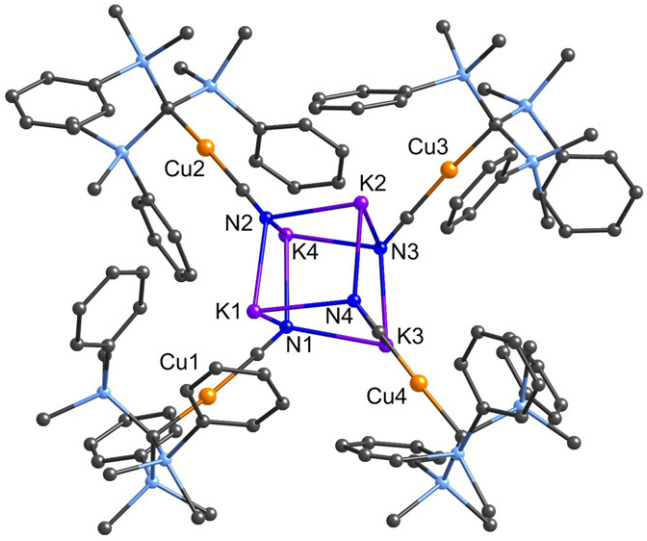

Fig. 45. Molecular structure of $[(Me_2PhSi)_3CCuCNK]_4$ [80].

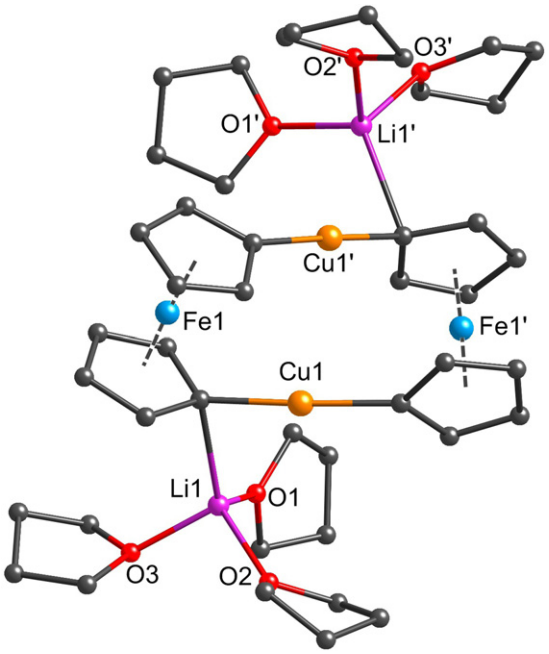

Fig. 46. Molecular structure of $[(1,1'\text{-Fc})_2Cu_2Li_2(THF)_6]$ [139].

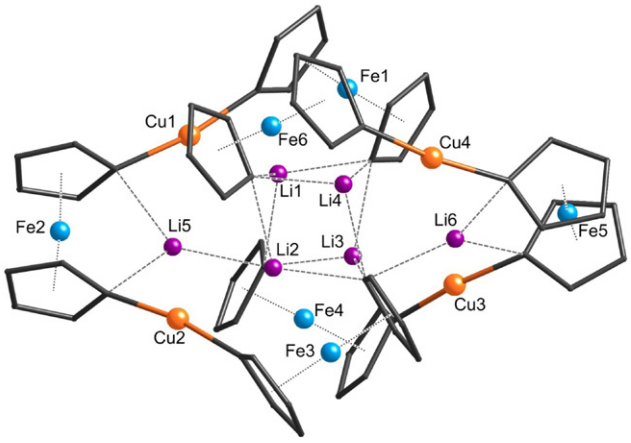

(a)

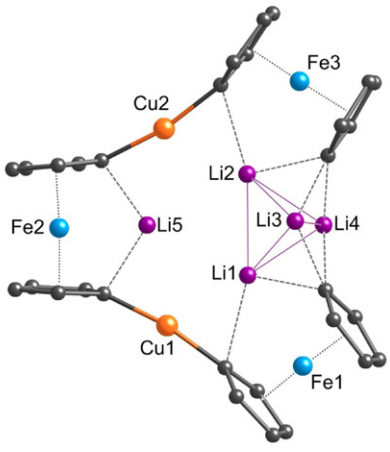

(b)

Fig. 47. (a) Molecular structure of the anion in $[(1,1'\text{-Fc})_6Cu_4Li_6][Li(THF)_4]_2$. (b) Cross-section of the anion, showing selective atoms only for clarity [139].

rings are close to parallel (tilt angle, 2.9°), and are much nearer to staggered than eclipsed in conformation. This results in the ferrocenylene units lying almost orthogonal to one another (torsion angle, 81.44°). However, despite the formation of a $(1,1'\text{-Fc})_2Cu_2$ ring, the Cu–Fe distances are fairly long (3.220, 3.522 Å) and there is no evidence of any Cu–Fe interactions.

In contrast to other dimeric lithium homocuprates, the lithium cations in $[(1,1'\text{-Fc})_2Cu_2Li_2(THF)_6]$ lie outside the central $(1,1'\text{-Fc})_2Cu_2$ dimeric ring, and are associated to a ferrocenylene carbanion *via* a 2.266(6) Å Li–C bonding interaction. Each of the lithium atoms is additionally coordinated by three THF molecules. The tetrahedral twist of the two ferrocenylene units and the Cp–Cu–Cp linkages, and the placement of the two $Li(THF)_3$ moieties results in the complex having conformational chirality. This twisting of the two ferrocenylene units was attributed to steric forces within the complex.

The use of *n*BuLi/TMEDA as the base yielded crystals of the closely related complex $[(1,1'\text{-Fc})_6Cu_4Li_6][Li(THF)_4]_2$. The complete reaction of the dilithioferrocene with copper(I) to form the quintessential R_2CuLi type organocuprate has therefore not fully proceeded, there being two less copper centers in the cluster than requisite. Of the twelve carbanion centers on the six ferrocenylene units present, eight are coordinated to both copper and lithium centers and can thus be considered lithium cuprate units, whereas the remaining four are solely coordinated to lithium centers and are best considered standard organolithium units. The anion can be regarded as being constructed from two $[(1,1'\text{-Fc})_3Cu_2]^{4-}$ units assembled perpendicular to one another around a central Li_4 core, with two additional lithium cations bridging the Cp rings of the dicuprated ferrocenylene units (see Fig. 47). Within the $[(1,1'\text{-Fc})_3Cu_2]^{4-}$ units the C–Cu–C bond angles approach linearity, mean 169.56°, and Cu–C distances (mean 1.915 Å) are comparable to those observed in $[(1,1'\text{-Fc})_2Cu_2Li_2(THF)_6]$.

7. Concluding remarks

The quest to understand the structures of organocuprates, and thus to shed light upon the origins of their unique synthetic applications, has engaged chemists ever since these species were first reported over fifty years ago. As detailed in this review, a number of different spectroscopic and characterizational techniques have been employed in this pursuit including X-ray crystallography, multinuclear and multi-dimensional NMR, EXAFS, XANES, molecular mass measurements, mass spectrometry, Infra-red studies and computational investigations. In this paper we have mainly focused upon the solid-state structures of organocuprates as determined using X-ray crystallography, although these have been correlated to solution structures using NMR or other reported solution studies wherever possible.

Solid-state structural characterization has regularly been shown to be an important starting point in the understanding of organocuprate reagents as it can provide a key reference point to assist in interpretation of often complicated NMR spectrum and also proffers a starting model on which theoretical calculations can be based. One particular example of the key importance of solid-state structural determination was in the controversy regarding the nature of higher order cyanocuprates: it was only after the publication of the solid-state structures of $[t\text{Bu}_2\text{Cu}][Li_2(CN)(PMDETA)_2(THF)_2]$ and $[(C_6H_4(CH_2NMe_2)\text{-}2)_2CuLi_2(CN)(THF)_4]_\infty$ that these species were universally accepted as existing primarily as cyano-Gilman type reagents ($R_2CuLi.LiCN$) rather than true higher order species in which the cyano group remained bound to the copper center (see Section 3.2) [86].

Nevertheless it is important to acknowledge the critical role played by other characterizational methods, especially NMR spec-

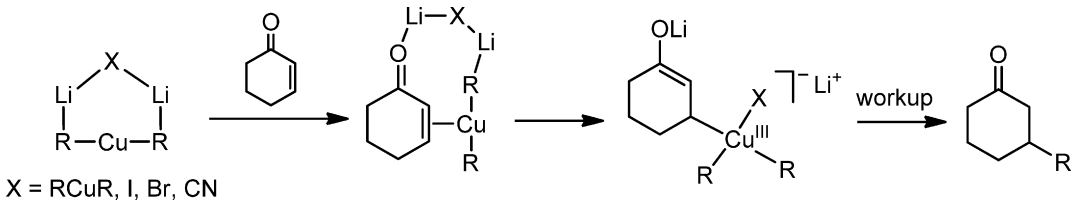

Scheme 11. Postulated mechanism for lithium homocuprate conjugate addition reactions.

troscopy [18]. In recent years in particular there have been many advances in the understanding of reaction mechanisms involving organocuprates which have been achieved using newly developed NMR-based techniques (such as low temperature rapid injection NMR methods [140]). These have enabled not just the identification of the resting states and solution equilibriums of organocuprates, but also in some cases the characterization of their reaction intermediates with substrates. For example, in conjugate addition reactions to enones the initial π-complex between the enone and the organocuprate has been identified [141] and more recently several Cu(III) intermediate complexes have been spectroscopically characterized [18,142–144]. These studies have subsequently allowed for a much more detailed reaction mechanism of the conjugate addition reaction of organocuprates to be proposed (Scheme 11).

The structural studies presented in this review demonstrate the array of supramolecular aggregates formed by organocuprates, often based on the aggregation of linear cuprate anions with lithium or magnesium cations. The precise arrangement of the organo groups and metal centers within these supramolecular fragments is envisaged to be important in facilitating the subtle cooperation between the two different metal centers which is required for the desired reactivity of the organocuprate, and may also play a role in controlling the Cu(I)/Cu(III) redox potential. In addition, the structures of these supramolecular aggregates have been shown to be highly influenced by a range of factors such as the solvent system, the ratio of the different metal centers, the presence of additives or by-products such as lithium halides or cyanide groups, the steric and electronic properties of the organo group, and the replacement of some of the organo groups with heteroatom based dummy ligands.

Many of the studies presented herein and much of our current understanding still involves lithium diorganocuprates with simple phenyl or methyl organo groups. In recent years, several research groups including our own have sought to redress this resulting in, for example, the publication of the first solid-state structural characterizations of lithium organo-amidocuprates as well as the first Grignard-derived organocuprate structures. Nevertheless, as is evident from this review there is still a paucity of data on many classes of organocuprates including those with metal centers other than lithium and also many categories of hetero organocuprates. Therefore it is imperative that we are not complacent based on recent successes and continue to work to fully unravel the intricacies of these important reagents.

References

[1] R. Reich, C.R. Hebd, Seances Acad. Sci. 177 (1923) 322.
[2] H. Gilman, J.M. Straley, Recl. Trav. Chim. Pays-Bas 55 (1936) 821.
[3] M.S. Kharasch, P.O. Tawney, J. Am. Chem. Soc. 63 (1941) 2308.
[4] H. Gilman, R.G. Jones, L.A. Woods, J. Org. Chem. 17 (1952) 1630.
[5] S. Pasynkiewicz, J. Poplawska, J. Organomet. Chem. 282 (1985) 427.
[6] H.O. House, W.L. Respess, G.M. Whitesides, J. Org. Chem. 31 (1966) 3128.
[7] G.M. Whitesides, W.F. Fischer, J. San Filippo, R.W. Bashe, H.O. House, J. Am. Chem. Soc. 91 (1969) 4871.
[8] E.J. Corey, G.H. Posner, J. Am. Chem. Soc. 89 (1967) 3911.
[9] N. Krause, Modern Organocopper Chemistry, Wiley-VCH, Weinheim, 2002.
[10] R.J.K. Taylor, Organocopper Reagents: A Practical Approach, Oxford University Press, Oxford, 1994.
[11] D.S. Surry, D.R. Spring, Chem. Soc. Rev. 35 (2006) 218.
[12] N. Krause, S. Thorand, Inorg. Chim. Acta 296 (1999) 1.
[13] N. Krause, A. Gerold, Angew. Chem. Int. Ed. Eng. 36 (1997) 187.
[14] J.T.B.H. Jastrzebski, G. van Koten, Structures and reactivities of organocopper compounds, in: N. Krause (Ed.), Modern Organocopper Chemistry, Wiley-VCH, Weinheim, 2002, p. 1.
[15] P.P. Power, Prog. Inorg. Chem. 39 (1991) 75.
[16] S. Woodward, Chem. Soc. Rev. 29 (2000) 393.
[17] E. Nakamura, S. Mori, Angew. Chem. Int. Ed. 39 (2000) 3751.
[18] R.M. Gschwind, Chem. Rev. 108 (2008) 3029.
[19] R.G. Pearson, C.D. Gregory, J. Am. Chem. Soc. 98 (1976) 4098.
[20] J.A.J. Jarvis, R. Pearce, M.F. Lappert, J. Chem. Soc., Dalton Trans. (1977) 999.
[21] R.L. Kieft, T.L. Brown, J. Organomet. Chem. 77 (1974) 289.
[22] G. van Koten, J.G. Noltes, J. Chem. Soc., Chem. Commun. (1972) 940.
[23] G. van Koten, J.G. Noltes, J. Organomet. Chem. 82 (1974) C53.
[24] A.J. Leusink, G. van Koten, J.W. Marsman, J.G. Noltes, J. Organomet. Chem. 55 (1973) 419.
[25] G. van Koten, J.T.B.H. Jastrzebski, F. Muller, C.H. Stam, J. Am. Chem. Soc. 107 (1985) 697.
[26] G. van Koten, J.T.B.H. Jastrzebski, J.G. Noltes, J. Organomet. Chem. 140 (1977) C23.
[27] N.P. Lorenzen, E. Weiss, Angew. Chem. Int. Ed. Eng. 29 (1990) 300.
[28] M.M. Olmstead, P.P. Power, J. Am. Chem. Soc. 112 (1990) 8008.
[29] S.H. Bertz, G. Dabbagh, Tetrahedron 45 (1989) 425.
[30] H. Hope, P.P. Power, J. Am. Chem. Soc. 105 (1983) 5320.
[31] R.P. Davies, S. Hornauer, Chem. Commun. (2007) 304.
[32] A. Hubner, T. Bernert, I. Sanger, E. Alig, M. Bolte, L. Fink, M. Wagner, H.-W. Lerner, Dalton Trans. 39 (2010) 7528.
[33] M. John, C. Auel, C. Behrens, M. Marsch, K. Harms, F. Bosold, R.M. Gschwind, P.R. Rajamohanan, G. Boche, Chem. Eur. J. 6 (2000) 3060.
[34] M.M. Olmstead, P.P. Power, Organometallics 9 (1990) 1720.
[35] X. Xie, C. Auel, W. Henze, R.M. Gschwind, J. Am. Chem. Soc. 125 (2003) 1595.
[36] M. Niemeyer, Organometallics 17 (1998) 4649.
[37] A. Muller, B. Neumuller, K. Dehnicke, Angew. Chem. Int. Ed. Eng. 36 (1997) 2350.
[38] B. Neumuller, A. Muller, K. Dehnicke, Z. Anorg, Allg. Chem. 628 (2002) 100.
[39] E. Nakamura, S. Mori, K. Morokuma, J. Am. Chem. Soc. 119 (1997) 4900.
[40] C. Eaborn, P.B. Hitchcock, J.D. Smith, A.C. Sullivan, J. Organomet. Chem. 263 (1984) C23.
[41] H. Hope, M.M. Olmstead, P.P. Power, J. Sandell, X. Xu, J. Am. Chem. Soc. 107 (1985) 4337.
[42] S. Mori, E. Nakamura, Tetrahedron Lett. 40 (1999) 5319.
[43] P. Leoni, M. Pasquali, C.A. Ghilardi, J. Chem. Soc., Chem. Commun. (1983) 240.
[44] D.F. Dempsey, G.S. Girolami, Organometallics 7 (1988) 1208.
[45] G.G. Dubinina, J. Ogikubo, D.A. Vicic, Organometallics 27 (2008) 6233.
[46] G. Hallnemo, C. Ullenius, Tetrahedron 39 (1983) 1621.
[47] C. Ouannes, G. Dressaire, Y. Langlois, Tetrahedron Lett. 18 (1977) 815.
[48] H. Huang, C.H. Liang, J.E. Penner-Hahn, Angew. Chem. Int. Ed. 37 (1998) 1564.
[49] R.M. Gschwind, P.R. Rajamohanan, M. John, G. Boche, Organometallics 19 (2000) 2868.
[50] S.H. Bertz, A. Chopra, M. Eriksson, C.A. Ogle, P. Seagle, Chem. Eur. J. 5 (1999) 2680.
[51] B.H. Lipshutz, J. Keith, D.J. Buzard, Organometallics 18 (1999) 1571.
[52] B.H. Lipshutz, J.A. Kozlowski, C.M. Breneman, J. Am. Chem. Soc. 107 (1985) 3197.
[53] S.H. Bertz, G. Dabbagh, J. Am. Chem. Soc. 110 (1988) 3668.
[54] S.H. Bertz, A.S. Vellekoop, R.A.J. Smith, J.P. Snyder, Organometallics 14 (1995) 1213.
[55] E. Nakamura, S. Mori, K. Morokuma, J. Am. Chem. Soc. 120 (1998) 8273.
[56] C.M.P. Kronenburg, J.T.B.H. Jastrzebski, J. Boersma, M. Lutz, A.L. Spek, G. van Koten, J. Am. Chem. Soc. 124 (2002) 11675.
[57] C.M.P. Kronenburg, C.H.M. Amijs, J.T.B.H. Jastrzebski, M. Lutz, A.L. Spek, G. van Koten, Organometallics 21 (2002) 4662.
[58] M.D. Janssen, M.A. Corsten, A.L. Spek, D.M. Grove, G. van Koten, Organometallics 15 (1996) 2810.
[59] E.C. Ashby, J.J. Watkins, J. Am. Chem. Soc. 99 (1977) 5312.
[60] E.C. Ashby, J.J. Watkins, J. Chem. Soc., Chem. Commun. (1976) 784.
[61] D.L.J. Clive, V. Farina, P.L. Beaulieu, J. Org. Chem. 47 (1982) 2572.
[62] P.G. Edwards, R.W. Gellert, M.W. Marks, R. Bau, J. Am. Chem. Soc. 104 (1982) 2072.
[63] S.I. Khan, P.G. Edwards, H.S.H. Yuan, R. Bau, J. Am. Chem. Soc. 107 (1985) 1682.

[64] H. Hope, D. Oram, P.P. Power, J. Am. Chem. Soc. 106 (1984) 1149.
[65] M.Y. Chiang, E. Bohlen, R. Bau, J. Am. Chem. Soc. 107 (1985) 1679.
[66] H. Eriksson, M. Håkansson, Organometallics 16 (1997) 4243.
[67] G. van Koten, J.G. Noltes, J. Organomet. Chem. 174 (1979) 367.
[68] G. van Koten, J.G. Noltes, J. Am. Chem. Soc. 101 (1979) 6593.
[69] P. Jutzi, W. Wieland, B. Neumann, H.G. Stammler, J. Organomet. Chem. 501 (1995) 369.
[70] B.H. Lipshutz, R.S. Wilhelm, J.A. Kozlowski, Tetrahedron 40 (1984) 5005.
[71] T.A. Mobley, F. Müller, S. Berger, J. Am. Chem. Soc. 120 (1998) 1333.
[72] M.M. Olmstead, P.P. Power, J. Am. Chem. Soc. 111 (1989) 4135.
[73] S.H. Bertz, G. Dabbagh, X. He, P.P. Power, J. Am. Chem. Soc. 115 (1993) 11640.
[74] F. Olbrich, J. Kopf, E. Weiss, Angew. Chem. Int. Ed. Eng. 32 (1993) 1077.
[75] B.H. Lipshutz, Synlett (1990) 119.
[76] J.-P. Gorlier, L. Hamon, J. Levisalles, J. Wagnon, J. Chem. Soc., Chem. Commun. (1973) 88a.
[77] S.H. Bertz, J. Am. Chem. Soc. 113 (1991) 5470.
[78] C.S. Hwang, P.P. Power, J. Am. Chem. Soc. 120 (1998) 6409.
[79] C. Eaborn, S.M. El-Hamruni, M.S. Hill, P.B. Hitchcock, J.D. Smith, J. Chem. Soc., Dalton Trans. (2002) 3975.
[80] C. Eaborn, M.S. Hill, P.B. Hitchcock, J.D. Smith, Organometallics 19 (2000) 5780.
[81] F. Bosold, M. Marsch, K. Harms, G. Boche, Z. Kristallogr. - New Cryst. Struct. 216 (2001) 143.
[82] G. Boche, F. Bosold, M. Marsch, K. Harms, Angew. Chem. Int. Ed. 37 (1998) 1684.
[83] M.A. Carvajal, S. Alvarez, J.J. Novoa, Chem. Eur. J. 10 (2004) 2117.
[84] A. Gerold, J.T.B.H. Jastrzebski, C.M.P. Kronenburg, N. Krause, G. van Koten, Angew. Chem. Int. Ed. Eng. 36 (1997) 755.
[85] C.S. Hwang, P.P. Power, Bull. Kor. Chem. Soc. 24 (2003) 605.
[86] N. Krause, Angew. Chem. Int. Ed. 38 (1999) 79.
[87] T. Stemmler, J.E. Penner-Hahn, P. Knochel, J. Am. Chem. Soc. 115 (1993) 348.
[88] T.L. Stemmler, T.M. Barnhart, J.E. Penner-Hahn, C.E. Tucker, P. Knochel, M. Boehme, G. Frenking, J. Am. Chem. Soc. 117 (1995) 12489.
[89] H. Huang, K. Alvarez, Q. Lui, T.M. Barnhart, J.P. Snyder, J.E. Penner-Hahn, J. Am. Chem. Soc. 118 (1996) 8808.
[90] S.H. Bertz, K. Nilsson, Ő. Davidsson, J.P. Snyder, Angew. Chem. Int. Ed. 37 (1998) 314.
[91] S.H. Bertz, G.B. Miao, M. Eriksson, Chem. Commun. (1996) 815.
[92] J.P. Snyder, D.P. Spangler, J.R. Behling, B.E. Rossiter, J. Org. Chem. 59 (1994) 2665.
[93] J.P. Snyder, S.H. Bertz, J. Org. Chem. 60 (1995) 4312.
[94] R.M. Gschwind, X. Xie, P.R. Rajamohanan, C. Auel, G. Boche, J. Am. Chem. Soc. 123 (2001) 7299.
[95] A. Putau, K. Koszinowski, Organometallics 29 (2010) 3593.
[96] C.M.P. Kronenburg, J.T.B.H. Jastrzebski, A.L. Spek, G. van Koten, J. Am. Chem. Soc. 120 (1998) 9688.
[97] E. Nakamura, M. Yamanaka, N. Yoshikai, S. Mori, Angew. Chem. Int. Ed. 40 (2001) 1935.
[98] W. Henze, A. Vyater, N. Krause, R.M. Gschwind, J. Am. Chem. Soc. 127 (2005) 17335.
[99] S. Usui, Y. Hashimoto, J.V. Morey, A.E.H. Wheatley, M. Uchiyama, J. Am. Chem. Soc. 129 (2007) 15102.
[100] R.P. Davies, S. Hornauer, Eur. J. Inorg. Chem. (2005) 51.
[101] B.E. Rossiter, N.M. Swingle, Chem. Rev. 92 (1992) 771.
[102] E.J. Corey, D.J. Beames, J. Am. Chem. Soc. 94 (1972) 7210.
[103] G.H. Posner, C.E. Whitten, J.J. Sterling, J. Am. Chem. Soc. 95 (1973) 7788.
[104] S.H. Bertz, G. Dabbagh, G.M. Villacorta, J. Am. Chem. Soc. 104 (1982) 5824.
[105] E. Nakamura, M. Yamanaka, J. Am. Chem. Soc. 121 (1999) 8941.
[106] M. Yamanaka, E. Nakamura, J. Am. Chem. Soc. 127 (2005) 4697.
[107] S.H. Bertz, C.A. Ogle, A. Rastogi, J. Am. Chem. Soc. 127 (2005) 1372.
[108] H. Yamamoto, K. Maruoka, J. Org. Chem. 45 (1980) 2739.
[109] R.K. Dieter, T.W. Hanks, B. Lagu, Organometallics 11 (1992) 3549.
[110] J. Eriksson, Ö. Davidsson, Organometallics 20 (2001) 4763.
[111] J. Eriksson, P.I. Arvidsson, Ő. Davidsson, J. Am. Chem. Soc. 122 (2000) 9310.
[112] R.P. Davies, S. Hornauer, P.B. Hitchcock, Angew. Chem. Int. Ed. 46 (2007) 5191.
[113] P.P. Power, K. Ruhlandtsenge, S.C. Shoner, Inorg. Chem. 30 (1991) 5013.
[114] P. Reiss, D. Fenske, Z. Anorg, Allg. Chem. 626 (2000) 1317.
[115] R. Bomparola, R.P. Davies, S. Hornauer, A.J.P. White, Dalton Trans. (2009) 1104.
[116] P.C. Andrews, D.R. Armstrong, D.R. Baker, R.E. Mulvey, W. Clegg, L. Horsburgh, P.A. Oneil, D. Reed, Organometallics 14 (1995) 427.
[117] J. Haywood, J.V. Morey, A.E.H. Wheatley, C.Y. Liu, S. Yasuike, J. Kurita, M. Uchiyama, P.R. Raithby, Organometallics 28 (2009) 38.
[118] S.F. Martin, J.R. Fishpaugh, J.M. Power, D.M. Giolando, R.A. Jones, C.M. Nunn, A.H. Cowley, J. Am. Chem. Soc. 110 (1988) 7226.
[119] A.H. Cowley, D.M. Giolando, R.A. Jones, C.M. Nunn, J.M. Power, J. Chem. Soc., Chem. Commun. (1988) 208.
[120] A. Eichhofer, D. Fenske, W. Holstein, Angew. Chem. Int. Ed. Eng. 32 (1993) 242.
[121] S. Dubbaka, M. Kienle, H. Mayr, P. Knochel, Angew. Chem. Int. Ed. 46 (2007) 9093.
[122] M. Ito, D. Hashizume, T. Fukunaga, T. Matsuo, K. Tamao, J. Am. Chem. Soc. 131 (2009) 18024.
[123] C.M.P. Kronenburg, J.T.B.H. Jastrzebski, M. Lutz, A.L. Spek, G. van Koten, Organometallics 22 (2003) 2312.
[124] C.S. Hwang, P.P. Power, Organometallics 18 (1999) 697.
[125] F. Lopez, A.J. Minnaard, B.L. Feringa, Acc. Chem. Res. 40 (2007) 179.
[126] S.R. Harutyunyan, T. den Hartog, K. Geurts, A.J. Minnaard, B.L. Feringa, Chem. Rev. 108 (2008) 2824.
[127] T. Jerphagnon, M.G. Pizzuti, A.J. Minnaard, B.L. Feringa, Chem. Soc. Rev. 38 (2009) 1039.
[128] L.M. Seitz, R. Madl, J. Organomet. Chem. 34 (1972) 415.
[129] D.M. Knotter, W.J.J. Smeets, A.L. Spek, G. van Koten, J. Am. Chem. Soc. 112 (1990) 5895.
[130] D.M. Knotter, D.M. Grove, W.J.J. Smeets, A.L. Spek, G. van Koten, J. Am. Chem. Soc. 114 (1992) 3400.
[131] E.M. Meyer, S. Gambarotta, C. Floriani, A. Chiesivilla, C. Guastini, Organometallics 8 (1989) 1067.
[132] R. Bomparola, R.P. Davies, S. Hornauer, A.J. White, Angew. Chem. Int. Ed. 47 (2008) 5812.
[133] R.E. Mulvey, F. Mongin, M. Uchiyama, Y. Kondo, Angew. Chem. Int. Ed. 46 (2007) 3802.
[134] K.W. Klinkhammer, Z. Anorg, Allg. Chem. 626 (2000) 1217.
[135] H. Eriksson, M. Ortendahl, M. Håkansson, Organometallics 15 (1996) 4823.
[136] M. Håkansson, H. Eriksson, A.B. Ahman, S. Jagner, J. Organomet. Chem. 595 (2000) 102.
[137] A. Alexakis, J.E. Backvall, N. Krause, O. Pamies, M. Dieguez, Chem. Rev. 108 (2008) 2796.
[138] R. Fischer, H. Gorls, M. Westerhausen, Organometallics 26 (2007) 3269.
[139] R. Bomparola, R.P. Davies, T. Gray, A.J.P. White, Organometallics 28 (2009) 4632.
[140] E.R. Bartholomew, S.H. Bertz, S.K. Cope, M.D. Murphy, C.A. Ogle, A.A. Thomas, Chem. Commun. 46 (2010) 1253.
[141] S.H. Bertz, C.M. Carlin, D.A. Deadwyler, M.D. Murphy, C.A. Ogle, P.H. Seagle, J. Am. Chem. Soc. 124 (2002) 13650.
[142] T. Gartner, W. Henze, R.M. Gschwind, J. Am. Chem. Soc. 129 (2007) 11362.
[143] H.P. Hu, J.P. Snyder, J. Am. Chem. Soc. 129 (2007) 7210.
[144] S.H. Bertz, S. Cope, M. Murphy, C.A. Ogle, B.J. Taylor, J. Am. Chem. Soc. 129 (2007) 7208.